The Aeronautical Journal (2023), **127**, pp. 1065–1103
doi:10.1017/aer.2023.39

ROYAL AERONAUTICAL SOCIETY

SURVEY PAPER

Separated and vortical flow in aircraft aerodynamics: a CFD perspective

A. Rizzi*

Engineering Mechanics Department, KTH Royal Institute of Technology, Stockholm, Sweden
Email: rizzi@kth.se

Received: 15 December 2022; **Revised:** 21 March 2023; **Accepted:** 13 April 2023

Keywords: Aerodynamics; Vortex flow; Stalling characteristics; Swept wings; Slender wings; Not-so-slender wings; Part-span vortices; Pitch-up instability; forensic CFD; Aerodynamic design assessment; Lanchester Lecture; Wing fence

Abstract

In the early era of aviation, Frederick Lanchester was both an inventor and a theoretician driven by the need for a theory of flight that would reduce the guesswork in designing new aircraft. His book *Aerodynamics* in 1907 laid down the early foundations of such a theory. The theory with contributions from others, notably Ludwig Prandtl, was refined to become the basis for the sleek designs of WWII aircraft brought about with little guesswork. New technology changed aircraft design radically with the increased speed of jet propulsion reaching into the transonic range with nonlinear aerodynamics. In the late 1940s and early 1950s substantial guesswork returned to aircraft design. The legacy of Lanchester et al., however, lived on with the development of computational fluid dynamics (CFD) that could guide designers through nonlinear transonic effects. This article presents a historical sketch of how CFD developed, illustrated with examples explaining some of the difficulties overcome in the design of the first-generation swept-wing transonic fighters. The historical study is *forensic CFD* in search for the likely explanation of the designer's choice for the wing shape that went into production a long time ago. The capability of current CFD applied to the aerodynamics of aircraft with slender wings is surveyed. The cases discussed involve flow patterns with coherent vortices over hybrid wings and wings of moderate sweep. Vortex-flow aerodynamics pertains to understanding the interaction of concentrated vortices with aircraft components. Modern Reynolds-Averaged Navier-Stokes (RANS) technology is useful to predict attached flow. But vortex interaction with other vortices and breakdown lead to unsteady, largely separated flow which has been found out of scope for RANS. Direct simulation of the Navier-Stokes equations is out of computational reach in the foreseeable future, and the need for better physical modeling is evident. Both cruise performance and stalling characteristics are influenced by strong interactions. Two important aspects of wing-flow physics are discussed: separation from a smooth surface that creates a vortex, and vortex bursting, the abrupt breakdown of a vortex with a subsequent loss of lift. Vortex aerodynamics of not-so-slender wings encounter particularly challenging problems, and it is shown how the design of early-generation operational aircraft surmounted these difficulties. Through use of forensic CFD, the article concludes with two case studies of aerodynamic design: how the Saab J29A wing maintains control authority near stall, and how the Saab J32 mitigates pitch-up instability at high incidence.

Nomenclature

M	Mach number
M_∞	free-stream Mach number
Re	Reynolds number
Re_{cref}, Re_c	Reynolds number based on wing reference chord
C_p	pressure coefficient
C_m	moment coefficient

A version of this paper was presented for the 2021 Royal Aeronautical Society Lanchester Lecture.
*Emeritus Professor of Aeronautics

C_L	lift coefficient
t/c	thickness-to-chord of wing section
CFD	computational fluid dynamics
UCAV	uninhabited combat aerial vehicle
RANS	Reynolds-Averaged Navier-Stokes
DNS	direct numerical simulation (of the Navier-Stokes equations)
LES	large eddy simulation
WRLES	wall-resolved large eddy simulation
WMLES	wall-modeled large eddy simulation
DES	detached eddy simulation
VLM	vortex lattice model
HALE	high altitude, long endurance
LERX	leading edge root extension
VG	vortex generator
VFE	vortex flow experiment
ACA	Advisory Committee on Aeronautics (UK)
NACA	National Advisory Committee on Aeronautics (USA)
NASA	National Aeronautics and Space Administration
NATO	North Atlantic Treaty Organization
RTO	Research and Technology Organization
STO	Science and Technology Organization
CAWAPI	Cranked Arrow Wing Aerodynamics Program, International
ITAR	International Traffic in Arms Regulations
AVT	atmospheric vehicle technology
AR	wing aspect ratio
AIAA	American Institute of Aeronautics and Astronautics

Greek symbols

α	angle-of-attack
Λ	wing sweep angle

1.0 Introduction

Separated and vortical flow occurs over every aircraft in flight. At optimum performance of low-speed aircraft, the airflow separates from the trailing edge of its unswept wing. The swept wings of high-speed aircraft often induce leading-edge separated flow that develops into vortices. Through interactions with the airframe, the separation-induced vortices affect the overall vehicle performance, stability and control. The effects can either be favourable or adverse, prompting Elsenaar to term the vortex the 'beauty and the beast in aerodynamics' in his Lanchester Lecture [1]. Luckring, in his Lanchester Lecture [2], presents a comprehensive survey of the discovery and prediction of vortex-flow aerodynamics.

The story begins in the last decade of the 1800s when Frederick Lanchester speculated correctly on the vortex theory of lift and the nature of the shear-layer wake shed from the trailing edge of a wing. In a sense one can claim that the study of vortex-flow aerodynamics began then with Lanchester. The theoretical model that evolved over the next three decades was linear and pertained to trailing-edge separation.

The flow physics of separation-induced leading-edge vortices is more complex and the theoretical models are nonlinear. Therefore, until the past decade or so, prediction of airframe aerodynamics involving such vortices has been anchored in experimental data. Theoretical modeling beginning in the 1950s and CFD simulations from the 1980s have also greatly expanded our understanding of these flows.

On a broad-brush canvas of vortex-flow aerodynamics, this article attempts to cast a historical perspective on the theoretical modeling of vortices from wing edges as it developed over the past century. Such a blanket approach allows us to parallel the historic achievements, along with the frustrations, of aerodynamic design during Lanchester's time with those of more recent times. Thus we begin with a brief discussion to establish the particular historical focus for the article.

https://doi.org/10.1017/aer.2023.39 Published online by Cambridge University Press

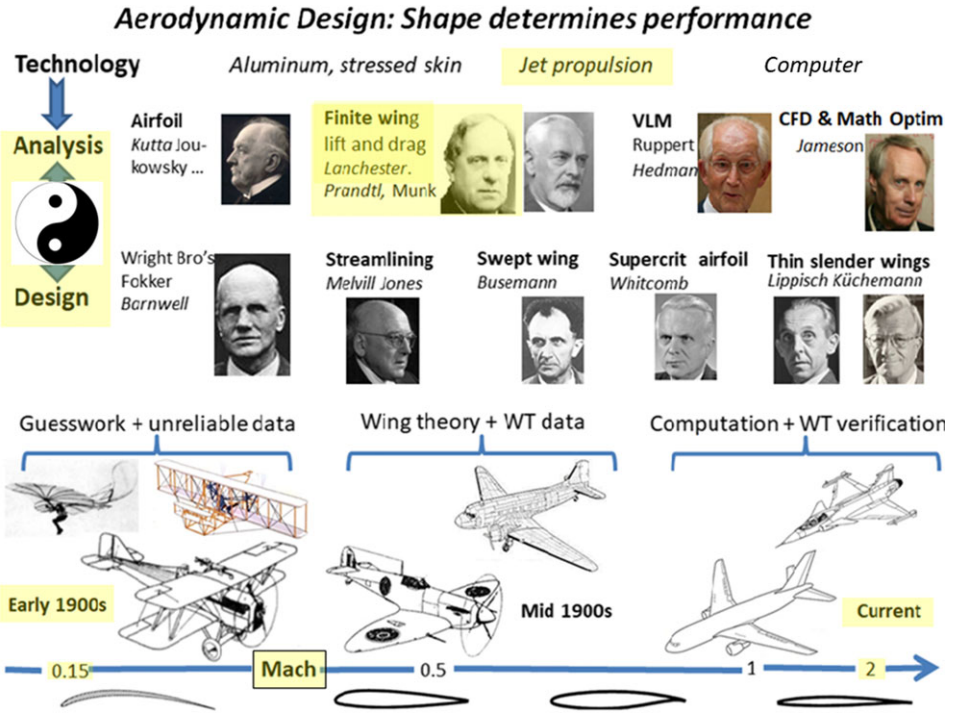

Figure 1. *100 Years of Aircraft Aerodynamic Design – from guesswork to optimal mathematical precision.*

1.1 One hundred years of aircraft design

Figure 1 presents a thumbnail history of the aerodynamic development of the airplane over the 20th century. Some of its significant contributors, Lanchester among them, are portrayed[1]. Giving just a glimpse of this rich history, the sketch offers a perspective in which to place Lanchester's contribution to vortex-flow aerodynamics, the computational modeling of which is the focus here.

The horizontal time line shows an order of magnitude growth in speed, the evolving shape of the wing profile, and the overall development of the aerodynamic shape. We have singled out three distinct eras. This development is driven by the arrival of new technologies such as stressed-skin construction, the jet engine and the digital computer. The advent of new enabling technology was exploited in the Yin-yang symbiosis between analysis methods crafted by theoreticians and design concepts pioneered by aircraft inventors in pursuit of performance.

1.1.1 Pioneering era – early 1900s

The first era, up to about 1918, was the birthing period of mechanical flight devices of many and varied shapes. The urge to design, build and take off outpaced the development of a sound theory of flight to guide design decisions. Thus, much aircraft design was carried out based on guesswork and unreliable data.

Figure 1 starts with Lilienthal and the Wright brothers, who built a wind-tunnel to obtain lift and drag data for wing sections. This was needed to estimate the engine power necessary for staying aloft. About the same time, the first mathematical models capable of predicting lift were being worked out by Kutta and Joukowski. Ludwig Prandtl's ground breaking boundary-layer theory enabled engineers

[1]The hundred-year sweep must necessarily be very abbreviated. Apologies to all those who contributed and are not mentioned.

https://doi.org/10.1017/aer.2023.39 Published online by Cambridge University Press

to better understand airflow quantitatively. Lanchester's book *Aerodynamics* in 1907 [3] laid down the early foundations of such a theory, and Ludwig Prandtl refined and mathematised it to become a truly useful quantitative tool for aerodynamic design.

Things started to come together towards the end of this era. The design of a new aircraft became a very structured undertaking following a script pioneered by Frank Barnwell in 1917 (see Anderson [4] for a full account).

The task of the aerodynamic designer is to shape the aircraft to meet the performance required for its mission: shape determines aerodynamic performance. Viewed from another perspective, designers use aerodynamic analysis to provide performance data of the shape that makes the best use of available technology.

Theory could now be combined with experiment to put data into the designer's hands, thereby eliminating much of the previous guesswork. For example, following from Lilienthal's research, the cross-sections of WWI aircraft wings were all thin with small nose radii. The design derived from a misinterpretation of the Reynolds number effect in the test data. In 1915 Hugo Junkers brought out an experimental monoplane aircraft with a thick wing, the J1, the world's first all-metal aircraft, although its nose radius was still rather small. In 1918 Anton Fokker gave his D-VII aircraft a thick aerofoil with large nose radius. That kept the airflow attached at high angles of attack and gave the plane superior climb and manoeuver performance.

1.1.2 Streamlining era – 1920s–1940s

Design work improved during the first decade of the second era, with the establishment of verified wing theory and reliable wind-tunnel data. The next couple of decades bring us from 100 mph contraptions of wood and fabric held together by bracing wires to the sleek shapes of 400 mph WWII fighters. Drag is the force the aerodynamic designer most wants to reduce in every design decision. Melvill Jones [5] proposed 'the streamline aeroplane' and showed the gains achievable by cleaning up the shapes to keep the boundary layer attached. The metamorphosis was made possible by technological infusions of materials, structural design and engine power. Lanchester-Prandtl lifting-line theory for lift and induced drag of wings made significant impact on the shapes. The RAF Spitfire's elliptical wing planform was drag-optimal by theory, and made it iconic. Boundary-layer theory coupled to an inviscid model, e.g. potential flow, does an excellent job in wing section design to this day, when a student's laptop can analyse a shape in minutes.

1.1.3 Modern era – 1950-present

The invention of the jet engine changed the game entirely and made planes fly faster and higher. Speeds close to Mach 1 had already been experienced by propeller-driven planes in dives and the deleterious 'compressibility effects' observed. High speed introduced the new design nemesis *wave drag* and centre-of-pressure travel.

Wing sweep was suggested by theorist Adolf Busemann [6], a pioneer in aerodynamics, already in 1935 as a means to reduce the drag associated with shock waves. Soon German aerodynamicists showed by experiment that his idea worked. Designs to limit wave drag brought about major changes in both planform and wing cross-section[2]. For swept planforms Whitcomb developed the *supercritical aerofoil* and the *area rule* to diminish wave drag at high speeds.

For supersonic flight even slenderer delta-shaped planforms were devised with very thin aerofoils. Conceptualising planform designs for a supersonic fighter aircraft in Germany during World War II, Alexander Lippisch [10] developed an experimental vehicle with a slender delta wing, the DM-1 glider,

[2]Meier [7] gives a very detailed account of the German work on this topic during the first half of the 1940s, including work on the area rule and what now is called the supercritical aerofoil. See also Sect. 2.4 of Hirschel et al. [8] as well as Rizzi and Oppelstrup [9] for more of this history during the 1940s.

https://doi.org/10.1017/aer.2023.39 Published online by Cambridge University Press

with a sweep angle of 60° that became something of a 'blueprint' for supersonic configurations. After the war Lippisch emigrated to the United States where the DM-1 evolved into the Convair XF-92A aircraft [2], and eventually into the F-102 Delta Dagger and F-106 Delta Dart. Delta wings, however, produce less lift and are prone to shed a vortex from their leading edge causing the configuration to fly poorly at low speed, close to stall when high incidence is needed for landing. In response to this problem, Dietrich Küchemann [11] pioneered the concept of designing for *healthy flow patterns* over slender configurations to achieve the desired performance, as e.g. with the Concorde.

New technology spawns new theory

The theoretical models that had served low-speed design so well were useless for speeds approaching Mach 1. The transonic speed range required non-linear models for aerodynamics. With the cold war on, enormous resources were poured into research and experiments to reach air superiority by speed and altitude, and in the late 1940s and early 1950s substantial guesswork returned to the design of transonic swept wings.

The legacy of Lanchester, namely the utility of solid theory to replace guesswork, however, lived on with the subsequent development of CFD. It was the growth of accessible computer power from 1950 onwards that enabled numerical solution of the non-linear partial differential equations of airflow to provide flow predictions at all speeds.

Computational models for transonic flow matured. From the eighties on, computer power and software could support not only flow prediction for a given shape, but also algorithmic shape optimisation. Antony Jameson's contributions to both CFD and shape optimisation can hardly be overestimated. Many, if not most, of today's computational fluid dynamics codes, such as the GNU public license SU2 [12] from Stanford University, are built from Jameson's ideas including the use of an *adjoint* equation to quickly compute the sensitivity of flow results to shape parameters.

1.2 Separation and vortical flow

Airflow past a body follows a script: the stream wets the body surface (attachment) and then detaches or separates from it at some location(s). Peake and Tobak [13] give a very detailed discussion of the distinction between attached and separated flows.

Following Hirschel et al. [8] a working definition of separation could be that vorticity from the boundary layer is convected away from the body surface at separation to form vortex layers and vortices. This is consistent with how Küchemann [14] put it – vortex layers and vortices, although not occupying much space in the flow field around and behind an aircraft, can be seen as 'the sinews and muscles of the fluid motion'. Indeed, the shedding of the 'starting vortex' from the trailing edge of the wing is the foundation of the classical theory of flight. Also Prandtl's lifting line analogy, later to develop into practical flow simulation methods such as the vortex lattice model, derives the velocity everywhere from strengths of vortical lamina and lines.

1.3 Organisation of paper

This paper surveys the capability of current CFD applied to the aerodynamics of aircraft with slender wings. The cases discussed involve flow patterns with coherent vortices over hybrid wings and wings of moderate sweep. Vortex-flow aerodynamics pertains to understanding the interaction of concentrated vortices with aircraft components. Both cruise performance and stalling characteristics are influenced. Two important aspects of wing-flow physics are discussed: separation from a smooth surface that creates a vortex, and vortex bursting, the abrupt breakdown of a vortex with a subsequent loss of lift. Vortex aerodynamics of not-so-slender wings encounters particularly challenging problems and it is shown how the design of early-generation operational aircraft surmounted these difficulties.

https://doi.org/10.1017/aer.2023.39 Published online by Cambridge University Press

The goal is to describe by examples our current understanding of separated and vortical flow in aircraft wing aerodynamics, to show the simulation capabilities of computation methods of different modeling level, and to demonstrate and to explain the relevant flow phenomena.

Section 2.0 recounts the reasons for why Lanchester is revered by today's aerodynamicists. Jet propulsion ushered in the high-speed era (see Section 3.0), when wings became swept and slender and their aerodynamics became nonlinear. The design of transonic swept wings, for lack of useful analytical tools, was carried out based on not very reliable wind tunnel data. The legacy of Lanchester, namely the utility of solid theory to rule out guesswork, however, lived on with the subsequent development of CFD. Section 4.0 briefly surveys the capability of current CFD applied to the aerodynamics of aircraft with slender wings with some discussion of physical modeling and vortex breakdown.

Using CFD as an analysis tool, Section 5.0 investigates the vortex aerodynamics of the not-so-slender Stability and Control Configuration (SACCON) uninhabited combat aerial vehicle (UCAV) concept and problems involved with incipient separation from its wing leading edge. We then follow Lanchester's example of applying theory to assess aircraft design. Section 6.0 uses forensic CFD analysis to seek motivations for design decisions on the swept-wing transonic fighters Saab J29 and J32. The task was to mitigate poor high-lift and stalling characteristics.

Lanchestrian symbiosis of theory and engineering paved the way to computerisation of mathematics into CFD. It helps bring together the analysis and design sides of aerodynamics. In its early days CFD was pejoratively interpreted as Colorful Fluid Dynamics. But those pictures now convey messages across the job-title spectrum from aerodynamicist to project manager and are indispensable in the concurrent, collaborative design efforts expended on new aircraft.

2.0 Lanchester legacy – linear wing theory

Both inventor and theoretician, Lanchester's aeronautics studies began in 1891 and continued roughly through 1918 when he conceived, designed, built and patented many practical devices. By building up a credible theory of flight he strove to find 'method in the madness' of aircraft design prevalent at that time and reduce the guesswork.

Having performed his own experiments, Lanchester is credited with developing the theory of circulation during the years 1892–1897, described in a paper, submitted to the Royal Society of London in 1897, that was rejected.

The 1897 paper essentially contained, as Lanchester said, the fundamental concepts of the circulation theory of lift (sustentation) and aerodynamic drag (resistance). They were presented in the first volume, entitled *Aerodynamics* [3], of the *Aerial Flight*, which was published ten years later, in 1907. In this book, Lanchester developed the relationship between circulation and lift for a wing and understood the connection between spanwise variation of lift and the development of a vortex wake.

Pioneering era perspective

Lanchester's time was a pioneering era for aeronautics. For perspective, we recall that the Wright brothers invented the airplane [15] with their first powered flight in December of 1903. Kutta in 1902 and Joukowski in 1906 and 1910 independently published what is now known as the Kutta-Joukowski condition. Prandtl published his boundary layer concept in 1904, and his lifting-line theory in 1911. Munk's dissertation [16] with the minimum-induced drag concept appeared in 1918. What we today know as fundamentals of aerodynamics were only being discovered during Lanchester's time [17].

This example reflects the theoretical knowledge at the time of Lanchester. The publication of *Aerodynamics* is right in the middle of the crucial theories that modeled the lift from circulation around a wing (see Table 1).

Von Kárman [24] reported that Lanchester was the first to address lift on a wing of a finite span. He developed the concept of a bound wing vortex connected to trailing vortices behind the wing and understood the significance of aspect ratio on wing performance. Circulation from the wing sheds into the trailing wake, which rolls up into a pair of trailing vortices about a wing span apart. He also put

https://doi.org/10.1017/aer.2023.39 Published online by Cambridge University Press

Table 1. *Aerodynamic theories at Lanchester's time*

Year	Theory	Author
1902	Kutta condition and lift	Kutta [18]
1904	Boundary layer concept	Prandtl [19]
1906	Lift is $L = \rho U \times \Gamma$	Joukowski [20]
1907	Publication of *Aerodynamics*	Lanchester [3]
1910	Formulation of Kutta-Joukowski condition	Joukowski [21]
1911	Lifting line theory	Prandtl [22, 23]

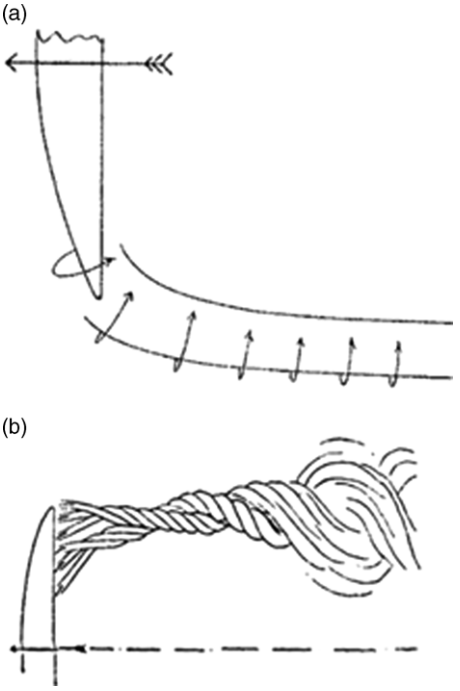

Figure 2. *Lanchester's circulation concept for lift (a) circulation sheds from wing into the trailing vortex, and (b) trailing wake vorticity coalesces into trailing vortex.*

forth the idea of tip vortices as the cause of the drag contribution known today as the lift-induced drag. Figure 2 illustrates some of his concepts.

A great debate broke out. Were the basic lifting line ideas Prandtl's or Lanchester's? Lanchester had given the annual Wilbur Wright Memorial Lecture 1926 and Prandtl was invited to give the 1927 lecture. Prandtl [25] acknowledged:

> In England you refer to it as "the Lanchester-Prandtl theory", and quite rightly so, because Lanchester obtained independently an important part of the results. He commenced working on the subject before I did, and this no doubt led people to believe that Lanchester's investigations, as set out in 1907 in his *Aerodynamics*, led me to the ideas upon which the aerofoil theory was based. But this was not the case. The necessary ideas upon which to build up that theory, so far as these ideas are comprised in Lanchester's book, had already occurred to me before I saw the book.
>
> At the same time, however, I wish it to be distinctly understood that in many particular respects Lanchester worked on different lines than we did, lines that were new to us, and that we were therefore able to draw many ideas from his book.

https://doi.org/10.1017/aer.2023.39 Published online by Cambridge University Press

Streamline body

Throughout *Aerodynamics*, Lanchester is careful to emphasise that, in all fluid motions, viscosity is of fundamental importance. In 1905, he was carrying out model glider experiments with the specific intention of estimating skin friction. Independently of Prandtl, Lanchester also proposed a boundary-layer concept.

A precursor to the work of Melvill Jones [5], he was fully aware of the benefits of a 'streamline body' defined in his book as

> A body that in its motion through a fluid does not give rise to a surface of discontinuity

where by 'discontinuity' he means the boundary between the outer flow and the dead water region formed by fluid that departs from the surface. Lanchester further noted:

> In all real fluids the influence of viscosity accounts for the departure, the departure being greater the less the viscosity.

He made a distinction between a massive separation and a local separation bubble, and he had a clear view of the formation of vorticity at the trailing edge of a lifting wing (see Fig. 2). Lanchester was well aware that separations destroy the flow, whereas the vortices are the cause of lift, required to realise 'aerial motion'. Clearly, the coming-of-age of theoretical aerodynamics began with Frederick Lanchester laying down the conceptual basis for the circulation theory of lift in the last decade of the 19th century [17]. But the quantitative formulas relating lift to circulation were developed during the first decade of the 20th century by Prandtl and Munk working independently, and without any knowledge of Lanchester's work.

2.1 Great divide: analysis vs. design

Lanchester was a firm believer in the maxim

> *There is nothing so practical as good theory*

long before Lewin [26] coined it in 1942. Why aerodynamic theory is so useful is easy to understand: it ideally provides a mathematical mapping from shape to aerodynamic performance. Knowledge of the (inverse of) this mapping allows the designer to go from a desired performance to a shape that yields it.

None of this was in place in aviation's very early years. Instead Jarrett [27] describes the situation as a *great divide* – the perceived lack of communication and understanding between those who made theoretical and scientific studies of aerodynamics but failed to comprehend the requirements of a practical airplane, and those who actually built and tried to fly airplanes but lacked scientific expertise.

Aviation's 'great divide' between mathematical theoreticians and practising designers and engineers persisted into the interwar years. In 1936, in the preface to the 'Performance' volume of the second edition of his book *Airplane Design*, Edward P. Warner, the head of aerodynamics at NACA Langley, summed up the status at that time:

> . . . the most important features of the decade [i.e. 1927–1936] in applied aerodynamics have been the provision of wind tunnels allowing tests to be made substantially under full-scale conditions, and an enhanced recognition by engineers of the practical usefulness of basic aerodynamic theory. In 1927, except for an occasional and gradually increasing use of induced-drag formulas, the typical designer thought of himself as having very little use for the offerings of the mathematicians, and he had very little disposition even to inquire into their application to his own work.

The designer is much more disposed in that direction now because CFD is helping to bridge this gap. It is no longer the mathematician's hard-to-understand equations that confront the designer, but the colorful

https://doi.org/10.1017/aer.2023.39 Published online by Cambridge University Press

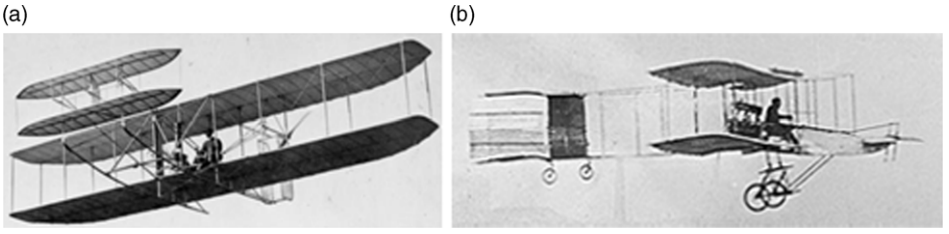

Figure 3. *Wright and Voisin flying machines: (a) Wright Model A [27] (with permission) and (b) Voisin biplane.*

graphics output of CFD software that visualises what is taking place in the flowfield. This makes it easier for the engineer on one side of the gap to respect and appreciate the techniques and efforts of the engineer on the other side without a deep knowledge of that person's expertise. CFD developers and practitioners need not become aircraft designers, but they must *communicate* efficiently with the design engineers.

2.2 Assessing aircraft – Wright and Voisin flyers

Lanchester had his feet planted on both sides of the gap. This is illustrated here by his analysis of the aerodynamic drag for the top-of-the line US and European flying machines of the day, the Wright Model A and the Voisin biplane (see Fig. 3).

Between 1904 and 1908 there was fierce competition between European aviation experimenters attempting to achieve powered heavier-than-air flight. The 1907 Voisin biplane was the first successful powered aircraft designed by aeronautical engineer and manufacturer Gabriel Voisin. French aviator Henri Farman made the first heavier-than-air flight lasting more than a minute in Europe, and also the first full circle. The airplane enjoyed widespread success, and around 60 planes were built.

During the summer of 1908 Lanchester had witnessed both types of aircraft in flight in France, the former piloted by Wilbur Wright at Le Mans, and the latter at Mourmelon le Grand near Chalons, flown by Henri Farman. On 8 December 1908 he read a paper before the Aeronautical Society of Great Britain entitled *The Wright and Voisin Types of Flying Machine. A Comparison* [28]. Lanchester writes:

> The author has collected sufficient data to give a consistent account of the performance of both machines and an intelligent comparison between them.

On hearing that the Wrights took no account of skin friction believing it to be negligible, Lanchester wrote: '*There is evidently considerable scope yet for guesswork*'.

Figure 4 is a reproduction for better legibility of Lanchester's drag breakdown for the two machines. Skin friction is assessed from wetted area and assumed friction coefficient. The influence of Voisin's very large empennage area is obvious. The largest contribution is labeled 'sustentation', i.e. lift induced drag. The Wright flyer has only 60% of the Voisin drag, since it is much lighter, at 350 kg for the Voisin's 550 kg.

2.3 Theoreticians divided – Rival theories in aerodynamics 1909–1930

Lanchester provided a conceptual basis for theory of lift, and Prandtl developed a quantitative model for lift. This circulation theory of lift, taking no account of viscosity but postulating its effect to be to set up the circulation, led to a theoretical divide located, as it were, in the English Channel. Acceptance of the Lanchester-Prandtl theory by 'Academia' came slowly. *The Enigma of The Aerofoil: Rival Theories in Aerodynamics 1909–1920* by David Bloor [29] tells the story in detail. Briefly stated, this is how the theory became accepted.

https://doi.org/10.1017/aer.2023.39 Published online by Cambridge University Press

	Wright. lb.	Voisin. lb.
Skin friction ξ = .01	40	60
Struts and wires	30	20
Aeronaut, motor, &c.	20	10
Radiator and tanks	5	25
Alighting gear	-	10
Sustentation(*)	60	100
	155	225

* Power expended aerodynamically

Figure 4. *Lanchester's drag breakdown [28]. Left column Wright Model A, right, Voisin biplane.*

Heavier-than-air flight came to be a widely known fact when the Wright brothers demonstrated it in Europe the summer of 1908. Many industrial countries were anxious to develop and exploit it for a variety of purposes; but a crucial problem remained – there was no agreement on how it worked from a basic physics point of view. This led the British to create a national Advisory Committee for Aeronautics (ACA) in 1909 to cure the awkward lack of understanding as to how such flight was possible. A plausible *quantitative* theory for the origin of the lift force was amiss. Dominated by veterans of the mathematics tripos tradition at Cambridge (see [30]), the ACA construed flight as a special case of fluid dynamics.

In contrast, the main German effort in this endeavour arose in the technical engineering schools, conducted primarily by mathematically sophisticated engineers working inductively from empirical research, foremost at Felix Klein's and Ludwig Prandtl's Göttingen University. The tradition that evolved in Göttingen was neither that of the pure mathematician nor that of the physicist. Neither rigor nor purity were central concerns, nor was it their primary goal to test the physical truth of their assumptions. Instead they tested their conclusions for *utility*. Indeed their approach was an early harbinger of modern applied mathematics as practiced today.

The dividing issue between the two schools became whether it makes any sense to explain the flight of airplanes in terms of *ideal* fluids whose viscosity is taken to be zero. This model cannot explain the *generation* of vortical air flow around a wing. The two communities followed diverging paths: the Cambridge School wanted to construct a fundamental theory of lift but did not help much in designing better wings, whereas the Göttingen School advanced wing design but could not explain how and why their theory worked. For those working within the British tradition, the inconsistency made the vortex theory of lift seem a non-starter. To truly *explain* lift, the idealising fiction of zero viscosity should be dropped. The Cambridge School held that nothing short of solving the Navier-Stokes equations would do. That came to mean waiting a very long time for a solution as discussed in Section 3.0. While Lanchester's theory consistently was rejected by the ACA, and the Cambridge School floundered on the Navier-Stokes equations, the Göttingen School developed/evolved circulation theory in a decade-long cumulative, puzzle-solving, and practically oriented modeling that produced Prandtl's finite-wing theory. In his Wright Memorial Lecture in 1927 Prandtl [25] stated:

> . . .I should like to point out that as a matter of fact we in Germany were better able to understand Lanchester's book when it appeared than you in England. English scientific men, indeed, have been reproached for the fact that they paid no attention to the theories expounded by their own countryman, whereas the Germans studied them closely and derived considerable benefit therefrom.

Figure 5 illustrates how the Prandtl model represents the flow around a wing. The reader interested in further discussion of the Göttingen School vis-a-vis the Cambridge School should see Chapter 3 of the book by Hirschel et al. [8].

https://doi.org/10.1017/aer.2023.39 Published online by Cambridge University Press

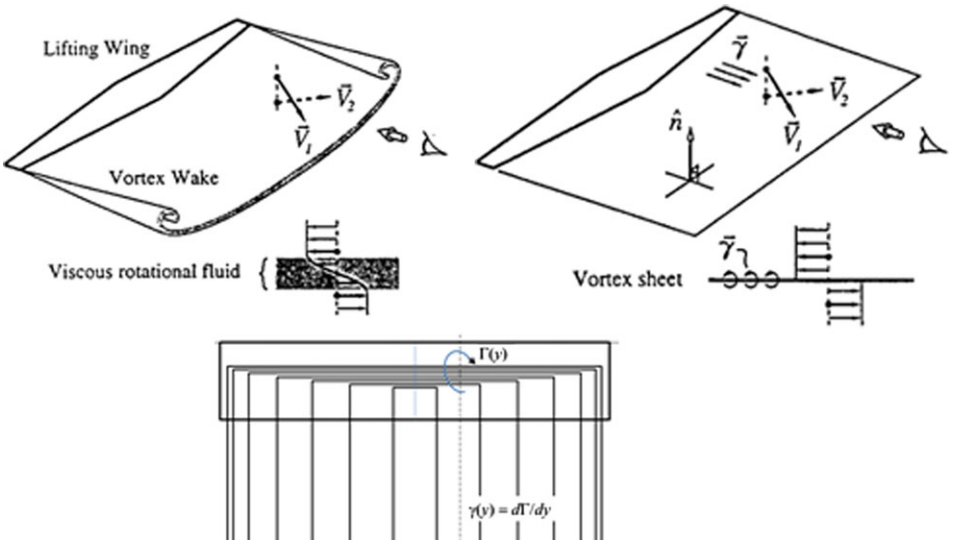

Figure 5. *Top left, the thin shear layer trailing from a straight wing, rolling up into the tip vortices. Right, the idealisation to a sheet of discontinuity with no roll-up. Bottom, the lifting-line model shedding streamwise vorticity to form the sheet.*

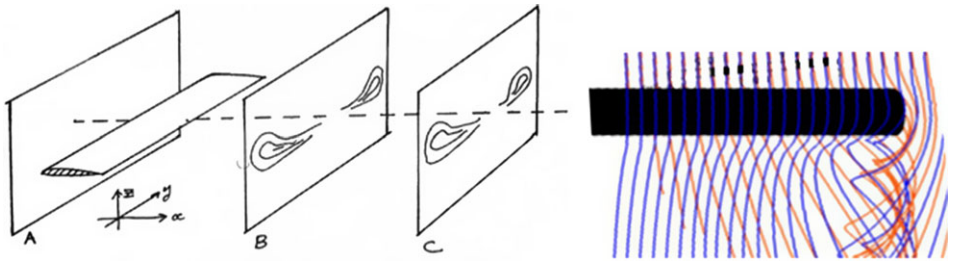

Figure 6. *Dispute resolved – Fage-Simmons measurements 1926: (left) WT experiment [29], and (right), CFD.*

2.3.1 Dispute resolved by Fage and Simmons measurements 1926

The dispute was put to rest when Fage and Simmons [31] in 1926 measured the circulation around a straight wing and its tip vortices. The results showed that the strength of vorticity leaving the tip equals the circulation around mid-section. The findings were published in 'An Investigation of the Air-Flow Pattern in the Wake of an Aerofoil of Finite Span' by the Royal Society of London. Figure 6 compares a drawing [29] of the Fage-Simmons measurements [31] with streamlines traced in a CFD computation.

In the face of this experimental verification, the Cambridge School 'accepted' the theory, if only begrudgingly. The wind-tunnel measurements may justify use of inviscid theory to represent real flow, but the finite-wing model cannot truly *explain* it because, within inviscid theory, the model had to postulate circulation, not deduce it. Nevertheless, acceptance of the inviscid model grew, and it was included in the 6th edition of Lamb's book *Hydrodynamics* (1932). Acceptance was far from complete, however. In his review of the book Sydney Goldstein [32], a prominent 'wrangler' of the Cambridge Mathematical Tripos, could not refrain from stating his misgivings about the appearance of circulation theory in the book.

https://doi.org/10.1017/aer.2023.39 Published online by Cambridge University Press

The real lesson learned from this rivalry is summed up in the aphorism coined by George Box some 50 years later:

All models are wrong, but some are useful.

3.0 High-speed era – nonlinear theory

Designs to limit wave drag brought about major changes in both planform and wing cross-section, but the lifting-line model which had served low-speed design so well was useless for speeds approaching Mach 1. The lack of analytical guidelines for improving performance left room for more guess-work. Not only was theory lacking, even wind tunnel testing was unreliable for transonic flow until the invention of slotted walls [33] in the late 1940s.

High speed requires the configuration to be slender and the cross-sections to be thin, which leads to separation from leading edges as well as trailing edges, resulting in much more complex vortex interactions than those that inspired Lanchester and Prandtl. See Rolls and Matteson [34] for the futility of studying the 35° swept wing of the F-86 Sabre at transonic speed with the Weissinger extension of the lifting-line theory, and comparing with flight tests.

Another invention, the programmable computer, appeared about the same time as the jet engine to clear a new path for aerodynamic analysis by enabling computational fluid dynamics.

3.1 CFD – the new analysis tool

Computational fluid dynamics (CFD) is the science of producing numerical solutions to a system of partial differential equations which describe fluid flow. Done by discrete methods it provides quantitative understanding of flow phenomena details which can then be used to improve upon engineering design. Essentially what the Cambridge School was holding out for in the 1920s was CFD, specifically for RANS, which only came about the better part of a century later. Figure 7 tells the story in a historical sketch over seven decades of CFD development juxtaposed with the evolution of supercomputing. The figure also includes select aircraft (first flight date) and collaborative CFD assessment ventures (green text).

Rizzi and Luckring [35] have presented the historical development of CFD in considerable detail so a brief account suffices here. Our focus begins in the late 1940s, before the first ‘knee’ in the S-shaped curve, when computers and numerical analysis were in their early days and progress was slow. What was not slow was the development of high-speed aircraft. With the cold war on, enormous resources were poured into research and experiments to reach air superiority by speed and altitude. Taking Saab development as an example, the J29 Tunnan was the first European swept wing fighter in service and made its maiden flight in 1948. Only seven years later the double-delta J35 Draken flew at Mach 2, and most fighters in service today fly neither much faster nor higher. The 1960s saw rapid development in numerical modeling fueled by growing computer power which caused the development curve to turn abruptly upwards.

3.1.1 Numerical modeling

The growth of computer power from 1950 onwards enabled CFD software development for flow predictions at all speeds. The impact was felt decisively from the 1960s when machines such as the IBM 7090 and later the IBM System 360 and the Control Data CD 6600 made high-performance computing accessible to engineers. The Vortex-Lattice Model (VLM) development of the lifting-line theory into working computer code was pioneered independently by Rubbert [36] at Boeing in Seattle and by Hedman [37] at FFA in Stockholm. It became a non-dispensable tool used to this day for low-speed analysis and design, also incorporating the effects of aero-elastic deformations. While the model was formulated decades

https://doi.org/10.1017/aer.2023.39 Published online by Cambridge University Press

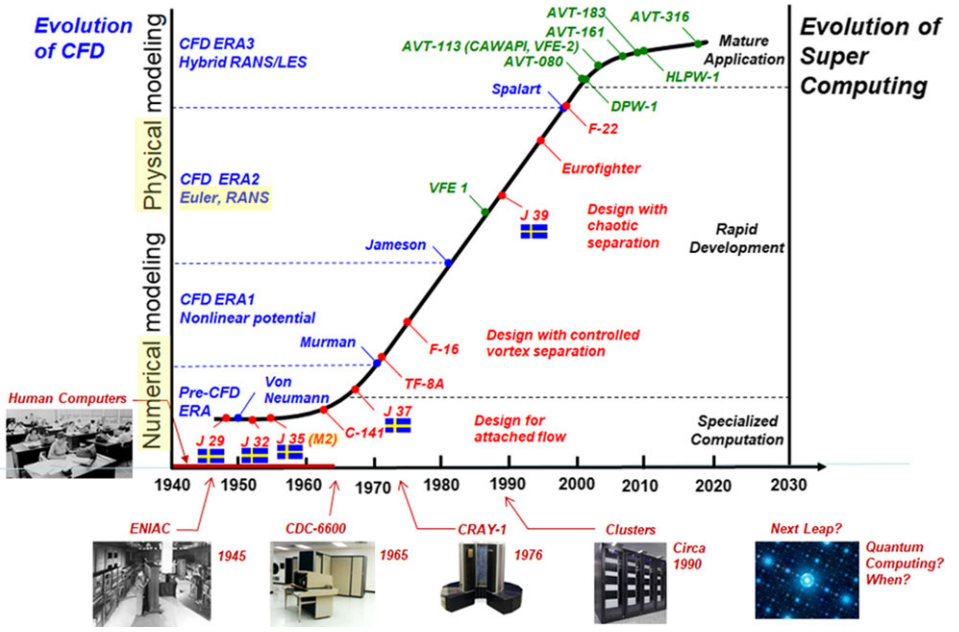

Figure 7. *Seven decades of CFD. (a) Red text aircraft; blue text numerics; green text assessment ventures.*

before, only with the availability of large memory machines and a software environment with Fortran and numerical libraries could a useful digital VLM implementation become a reality.

During the rapid development period, Rizzi and Engquist [38] reviewed the simulation work of primarily nonlinear phenomena: shocks, vortices and separation. The numerical modeling for computing discontinuous discrete solutions was highlighted. This brought in the grid generation aspects needed to resolve such phenomena and the mapping of the computational methods onto the computing hardware of the day. Their review concluded with a number of computed examples exemplifying the status of CFD, circa 1985, for computing such nonlinear vortical flow phenomena. Recently also the Lanchester Memorial lectures have focused on vortical flow, see J. Luckring [2] and A. Elsenaar [1]. In addition, Vos et al. [39] extensively reviewed, from a European perspective, the RANS technology for numerous problems in aircraft design up to about the year 2000, the start of the second knee in the curve.

The first two decades of this century, labeled ERA-3 in Fig. 7, saw the transition from vector computers with exotic hardware to mature application of scientific cluster-parallel computing. The period has also seen a *decline* in the growth rate of computing hardware capacity to meet the demands of physical modeling. Ever smaller scales in unsteady flows must be resolved to accurately represent extended regions of turbulent flows. For such studies the physical model of choice has been a hybrid RANS/LES simulator, initiated by Spalart [40] in 1997. Much needed validation and uncertainty quantification efforts have accompanied the shift in high-end CFD from RANS to higher fidelity models.

Throughout the decades, CFD development has taken the form of climbing a ladder of ever-increasing fidelity in physics simulation. Along the way, the ability to represent geometric complexity for aircraft applications has expanded, enabled by advancements in high performance computers and software libraries for parallel computing.

3.1.2 Physical modeling

The three past decades of developing RANS methods have produced very effective aeronautical CFD tools. They have also brought about the maturation of direct numerical simulation (DNS) methods for

https://doi.org/10.1017/aer.2023.39 Published online by Cambridge University Press

studying the physics of turbulence and transition without modeling. RANS technology today adequately predicts forces and moments for cruise conditions when the flow field is steady and the turbulent boundary layer remains attached over the aircraft surface [35] – the same conditions for which inviscid theory coupled with the boundary-layer equations are valid. Near-wall turbulence models suffice to treat this class of flow to required engineering precision.

Satisfactory predictions are also made when a vortex is shed from a sharp-edged swept wing and remains concentrated over the vehicle. The relevant vortical flow details remain large scale, and the turbulence-scales have only insignificant effects on the aerodynamic forces.

However, in some circumstances separated transitional and turbulent flows set aerodynamic limits for an aircraft flight envelope. The stalling characteristics encountered as maximum lift is approached is information the designer needs. Such predictions become less reliable, however, when the turbulent boundary layer separates before the tail of the vehicle and becomes unsteady over its surface. The turbulence is no longer wall-bounded and RANS turbulence models operate in flowfields for which they were not calibrated. Thus, many of these flows remain difficult to predict to an acceptable level of certainty with traditional CFD. RANS simulations of separated flows apparently have reached a level of diminishing returns as regards capability and certainty, as indicated by the knee in the development curve in Fig. 7 after 2000 [35]. Many CFD predictions of separated flows will require hybrid RANS/LES technology and even higher levels of physical modeling. The ubiquitous challenge here is turbulence, with transition equally challenging but in question only in relatively small regions and in special applications. Progress will be dependent on new ideas and their correct implementation. An assessment of the reliability of the physical modeling used in current CFD techniques is described in the following sections. For a fuller discussion of the progress and challenges of physical modeling, see Rizzi and Henningson [41].

3.1.3 Assessing modeling credibility

DNS studies can play a crucial role to advance the understanding of the flow physics. Recent advances in DNS methodology and increased computer capacity now allow aeronautical flow fields to be computed on first principles instead of by assumed models. DNS can accurately predict the separation, the laminar-turbulent transition and the often very sensitive interplay between these phenomena. DNS on the largest high-performance computers can compute flow situations typical of university wind tunnels to effectively act as a virtual wind tunnel.

For the foreseeable future, full-scale *Re* configurations are out of reach for DNS, and improved design tools will rely on progress in physical modeling. But the two communities, the DNSers and the modelers, are not on either side of some great divide. Instead, the DNS tools offer unprecedented quality and volumes of data to help the modelers, as the understanding of flow mechanisms simultaneously expands. Likewise, we see the engineering and academic communities rapidly joining forces in the quest for better theory, models, software and finally aerodynamics.

Collaborative assessment campaigns

In Fig. 7 ERA-3 was earmarked by mature applications of CFD to flying aircraft, and highlighted the need for assessing the credibility of the modeling. The goal is not only to obtain good agreement on a specific example, but to *get the right answer for the right reason*. The numerical answer may match, or miss, a measured result depending on how the modeled physics relate to those in the experiment.

The process of determining the accuracy of a model as a representation of the real world from the perspective of its intended use is a very demanding task. It involves the identification and quantification of the errors and uncertainties in the conceptual and computational models. For CFD calculations to add value to the credibility 'data base', the assessment teams must make sure that the solutions are reasonable and trustworthy, and stable with respect to variations in the input parameters for the software used. This demanding task requires a careful systematic approach to the whole process from geometric model to interpretation of computed quantities. To help, the European Research Community on Flow,

https://doi.org/10.1017/aer.2023.39 Published online by Cambridge University Press

Turbulence and Combustion (ERCOFTAC [42]) has published *Best Practice Guidelines for CFD* in various applications.

Although single-code/single-investigator CFD assessments will continue to advance our software, teamed and sustained collaborative campaigns offer significant benefits for advancing computational modeling. They bring diversity of opinion and numerical formulation along with the opportunity to assess numerical uncertainty. Examples are the AIAA Prediction Workshops, the STO-NATO AVT Task Groups and the National Aeronautics and Space Administration (NASA) Cranked Arrow Wing Aerodynamics Program, International (CAWAPI) series. Each of these campaigns has a unique aerodynamic focus that, in turn, stresses the particular underlying flow physics.

Unit problem

Collaborative assessment campaigns can help by the study of *reduced complexity* problems relevant to the aerodynamics of interest. The physics of many of the fundamental vortex flow phenomena, such as vortex breakdown, shock-vortex interactions and blunt leading-edge separation occur simultaneously and interact so it is difficult to find the effect of each. The scientific method proceeds to analyse by devising experiments focusing on one phenomenon at a time. The term *model problem* is much used for such experiments. However, it has a much wider connotation, and we use *unit problem* instead. Section 4.0 describes several examples of collaborative assessments of separated flow, unit problems included.

3.2 Swept and slender wings

Major driving forces for the rapid development of CFD during ERA-1 and ERA-2 were the needs for aerodynamic prediction methods for the transonic speed range where shock waves appear. Likewise, prediction capability is desirable for strong separated vortices which show up at large angles attack for highly swept wings. Appearing in the late 1940s and early 1950s were wings in slender configurations with swept leading edge. High sweep meant lower high-speed drag but also less lift. However, it was discovered that separation from a sufficiently swept leading edge created a stable vortex over the wing to enhance lift, and this effect is widely exploited in all designs. Flows with *coherent vortex separation* then lead to new nonlinear interaction phenomena, such as: vortex breakdown stall, shock-vortex interaction and shock-vortex-boundary layer interactions (SVBLI) of many variants.

Figure 8 makes this discussion more concrete by displaying representative aircraft in a chart with speed as Mach number M on the vertical axis and the sweep angle of the wing, typical of its speed class, on the horizontal axis. Subsonic straight-wing aircraft as one class, at the bottom left, encounter 'classical boundary layer separation' that leads to stall with increasing angle-of-attack, either by separation from the leading or trailing edge. See Hirschel et al. [8] for further discussion.

Jet fighters as early as the late 1940s (e.g., F-86), mid-Fig. 8, as well as airliners today, fly transonically with swept wings. Modern UCAV, such as the SACCON studied in Sec. 5, have wing sweep and aspect ratio to position them also in the second class of Fig. 8. In this condition a new phenomenon, shock stall, is brought on by shock waves interacting with the boundary layer. It hinders pressure recovery even more so that separation occurs at lower incidence angle than at subsonic flight. Also, swept wings are prone to tip stall, which could lead to a loss of aileron efficiency and pitch-up. That was an issue for aircraft like the B-47 as well as the F-86. The problems were solved by various 'fixes' like outer-wing-panel vortex generators (B-47), leading-edge slats (F-86) and the horizontal all-moving tail (F-86).

As demands for ever higher speed advanced, supersonic fighters appeared early in the 1950s, Fig. 8 right, requiring thin wings in slender configurations, a third class of aircraft. Supersonic aircraft included delta-wing applications such as the Convair F-106, the MiG 21, and the hybrid-wing Saab J35, Fig. 9.

The US fighters of recent times all have *hybrid wings* with highly swept inner wings, forebody strakes, or chines, coupled to outer wings with moderate sweep, and these two swept panels *mutually interfere* aerodynamically by design to produce more lift. The F-16XL, shown also in Fig. 9, is a good example of this.

https://doi.org/10.1017/aer.2023.39 Published online by Cambridge University Press

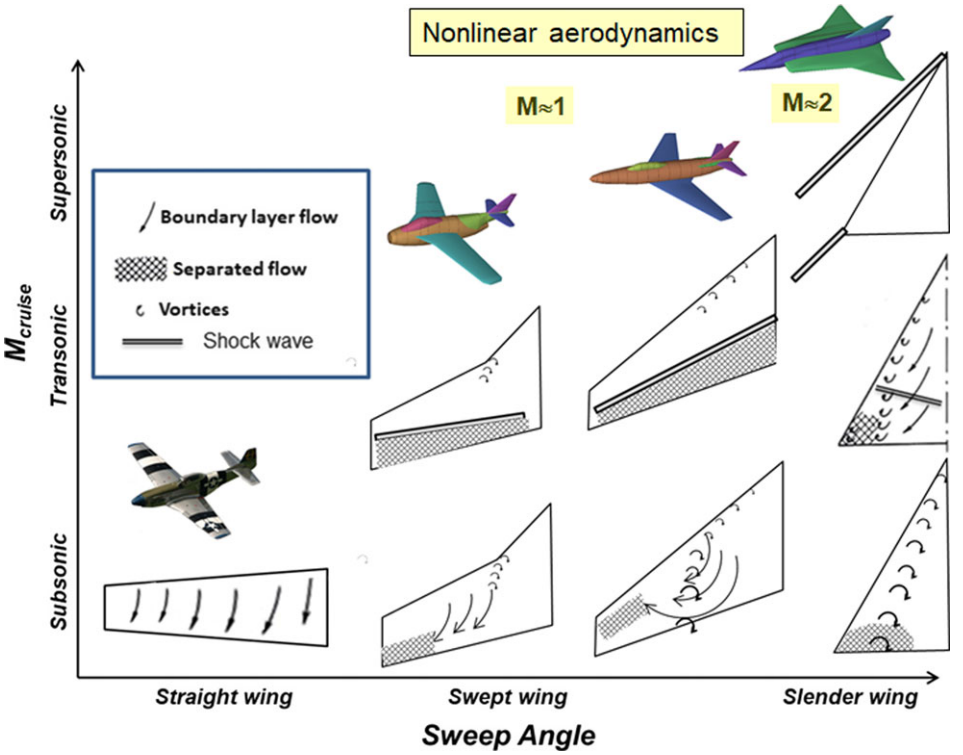

Figure 8. *Military aircraft separated flows.*

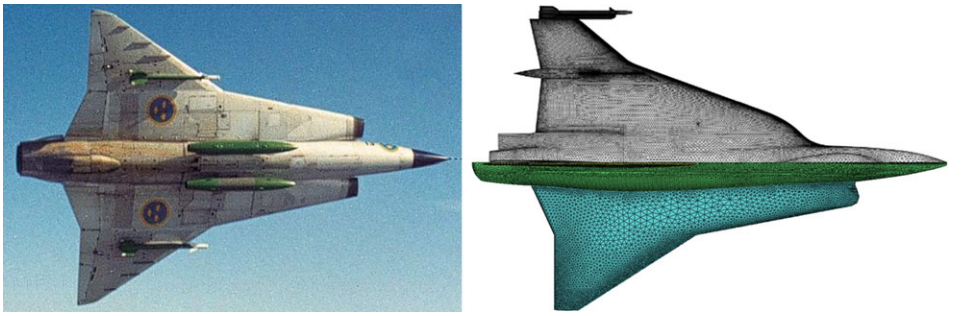

Figure 9. *Left, the Saab J35 in flight showing the three wing pressure side vortilons; right, planform views of the J35 (bottom) and the F-16XL (top).*

Hybrid wings

The Saab J35 Mach 2 fighter first flew in 1955. Its planform is compared with the modern F-16XL in Fig. 9, right. The inner wing needs to be 'joined' to the fuselage in a suitable way. The J35 inner wing is extended into the air intake whereas the F-16XL has an overall S-shape 'blend' with very sharp leading edge on the section connecting to the forebody, effectively a low-sweep LEX. Hybrid wings also undergo shock/boundary-layer interaction (SBLI) and leading-edge vortex separations. Hirschel et al. [8] explain and elaborate these types of phenomena, their modeling and computation, at book-length.

https://doi.org/10.1017/aer.2023.39 Published online by Cambridge University Press

Less lift on slender wings

An accurate expression for the estimation of the effects of sweep angle Λ, aspect ratio AR, and Mach number $M_\infty < 1$ on the subsonic lift-curve slope for thin wings reads

$$\frac{dC_L}{d\alpha} = \frac{2\pi AR}{2 + \sqrt{AR^2\left(1/\cos^2\Lambda - {M_\infty}^2\right) + 4}} \tag{1}$$

For example, for any sweep angle, low AR wings (say 1 or 2) have only about one half the lift-curve slope of large AR wings (say 10). The lift-curve of wings of AR 5 or 10 lose almost half their slope when sweep angle goes from zero to 50°. Thus swept and slender wings produce substantially less lift than straight wings, and pose a design challenge for the aircraft to land safely. One common compromise designers opt for then is the hybrid wing.

Let us now look more closely at three fundamental separation phenomena occurring in the scenarios described above.

3.2.1 Complex interactions with vortices

The broad range of vehicle classes and operating conditions result in a wide variety of separated flows that are important to military aircraft operations. Vortex flow aerodynamics dominate at higher angles of attack. Flow visualisation in water tunnels or with oil-flow in windtunnels gives useful information for interpretation of the vortex patterns. However, inference on forces and moments from the behaviour of the set of vortices is not straight forward.

Torsten Örnberg, aerodynamicist on the Saab J35 project, was a proponent of creating healthy flow in the Küchemann sense by controlling the vortices. Vortices should be kept from close interaction. When close they will rotate each other just like trailing wing-tip vortices sink by their mutual induced flow. Örnberg called this *vortex rotation* and concluded that rotations of more than about half a revolution over the wing led to breakdown and must be avoided. Vortices lose stability with the distance from their lift-off, so splitting can be effective. The J35 wing had three vortilons under the wing (see Fig. 9), which successfully delayed the suction side vortex breakdown. Örnberg had developed the idea on a study of clean delta wing flows but it met with little initial interest from Saab. He obtained a Swedish patent [43] just in time for Saab to have second thoughts, so the devices were considered for the J35 after detailed testing. More standard vortex generating fences on the suction side were found also to work when placed properly and led to a US patent [44]. But their supersonic drag was significant and they would have to be retractable. This was deemed too complex and the vortilons were chosen for final design. Figure 10 shows an artist's impression of the suction side vortex system, vortilons drawn dashed, from the Swedish patent brief. Next to it is an oil flow experiment with a J35 model showing the surface flow footprint of the numerous vortices.

Vortex-surface interactions include both the interactions between the primary vortex and the underlying wing that results in a secondary vortex, as well as the interactions of the primary vortex with a downstream component, such as the empennage. Each class of vortex interaction has its challenge for accurate computation, and each can include abrupt state changes, such as from a weak to a strong interaction. The next section discusses the main physics active in these interactions.

3.2.2 Separation and stalling characteristics

Wing sweep also brought disadvantages that made successful design very challenging. For example the spanwise pressure gradients induce spanwise flow of the boundary layer toward the tip. The resulting increase in boundary-layer thickness in the aft outboard region can, for thick wings in particular, promote tip stall with the accompanying adverse effects of pitch-up instability and controllability problems.

https://doi.org/10.1017/aer.2023.39 Published online by Cambridge University Press

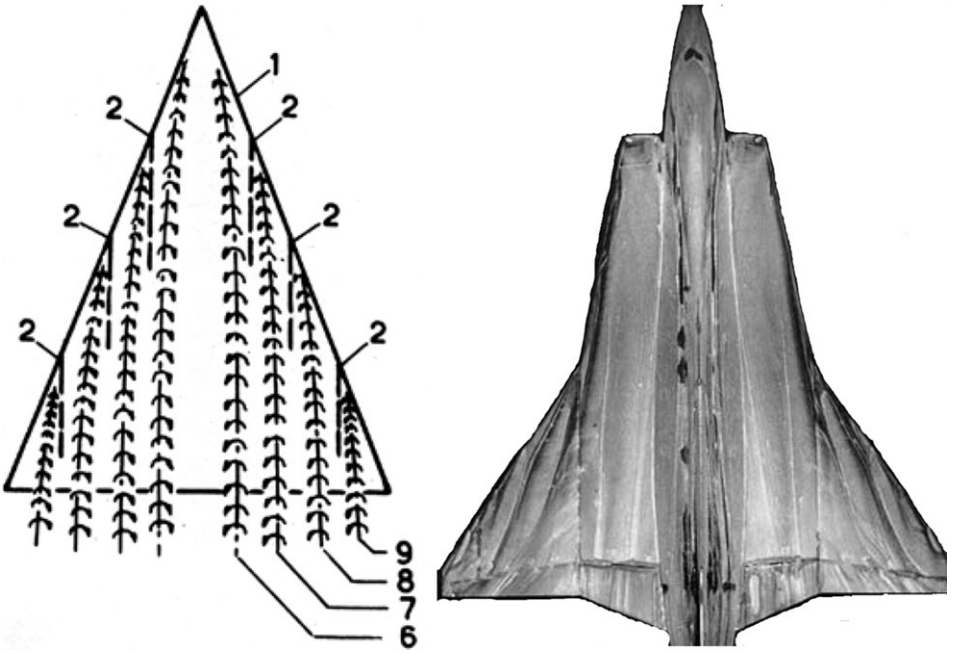

Figure 10. *Left, Örnberg's interpretation of the vortex system on a delta wing leeside with three vortilons. Right, oil-flow visualisation of the J35 vortex system.*

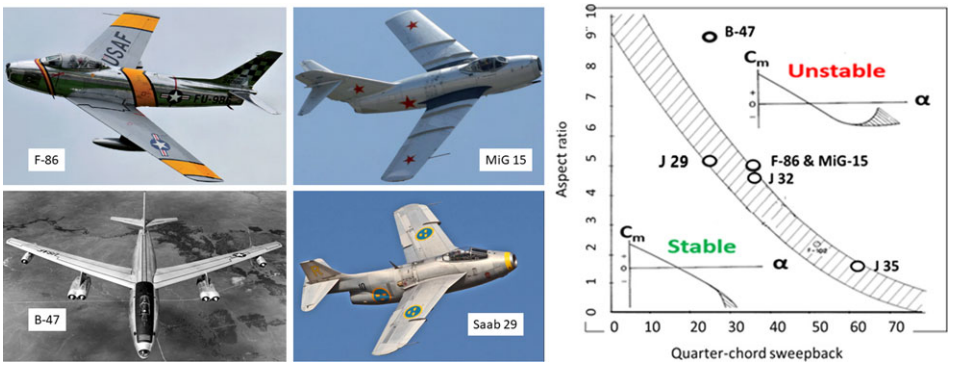

Figure 11. *Left: 1948 swept wing military aircraft. right, aspect ratio – sweep stability diagram.*

Pitch-up instability

All first-generation transonic swept-wing fighters, such as the North American F-86, the MiG-15, and the Saab J29, as well as the B-47 bomber, depicted in Fig. 11, left, encountered tip stall instability problems that required ingenious engineering solutions to overcome. Pitch-up was among the issues to be resolved, and in-flight stall characteristics were documented both for an F-86A [34] and the Saab J29 [45]. Rizzi and Oppelstrup describe the problems with these swept wings in their textbook [9] and explain in detail some of the solutions.

Separation on swept wings initially occurs over the tip sections. Flow separation and loss of lift aft of the centre of gravity usually result in a pronounced nose-up pitching moment. Summarising the results of wind-tunnel tests of swept-back wings, Shortal and Maggin [46] showed that whether or not instability would be obtained on a wing of given sweep depended primarily on aspect ratio. The stability boundary

https://doi.org/10.1017/aer.2023.39 Published online by Cambridge University Press

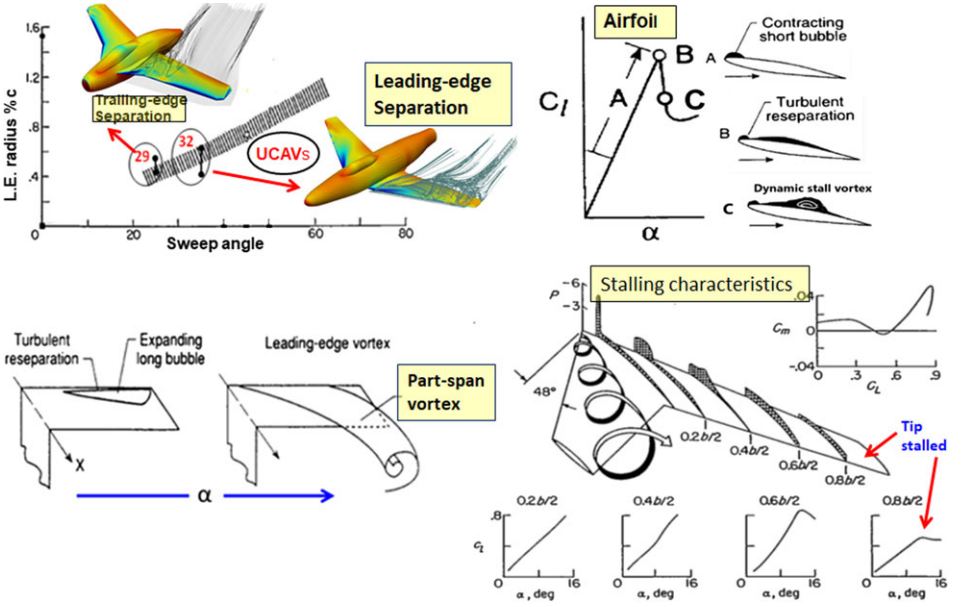

Figure 12. *Phenomenological notion of the physics occurring on leading-edge vortex formation. Top left, approximate boundary in terms of leading-edge radius and sweep angle for vortex formation [47]; top right, leading-edge stall on aerofoil [48]; bottom left, bubble separation into Ram's Horn vortex [48], right, stalling characteristics and pressure distribution on wing with tip stall [47].*

they constructed provides a general classification of the stability of any particular aircraft wing, in Fig. 11 right. It shows the combined effect of sweepback and aspect ratio on the shape of the pitching-moment curve. Both the tip-stalling tendencies and low values of attainable lift of swept wings constitute landing and take-off problems at low speeds requiring mitigation.

Incipient vortex separation

The sweep angle at which vortex flow develops and contributes to lift and/or pitch instability is related to the leading-edge radius of the wing. The leading-edge radius decreases rapidly with aerofoil thickness; hence, the thinner the wing, the lower the sweep angle at which vortex flow occurs. From wind-tunnel tests Furlong and McHugh [47] compiled, in Fig. 12 top left, an empirical boundary between wings which are subject to leading-edge vortex flow and those which are not.

Polhamus [48] summarised a succession of separation classes and a phenomenological notion of the physics which occur on leading-edge-stall aerofoils. Figure 12 top right shows the case relevant here. At some incidence angle α, a laminar separation bubble occurs at the leading edge and contracts with increasing α. After considerable contraction of the bubble, the pressure gradient in the leading-edge region suddenly separates the turbulent boundary layer aft of the short bubble re-attachment. This *turbulent reseparation*, creates an expanding *long bubble* and an abrupt loss of lift. The long bubble may, or may not, close before reaching the trailing edge. Visbal and Garmann [49] simulated a somewhat similar case with wall-resolved large eddy simulation (WRLES) and found vortical features in their solution that are compatible with what was just described. Such is the scenario for a straight wing; next add sweep.

With increasing sweep angle, three primary phenomena arise, in simplified form in Fig. 12 bottom left. The chordwise and spanwise distributions of surface pressure across the span increase toward the tip due, in part, to the spanwise variation of upwash associated with the vorticity of the swept-wing attached flow and wake. See, for example, the textbook [9]. The spanwise pressure gradient along the

https://doi.org/10.1017/aer.2023.39 Published online by Cambridge University Press

leading edge sweeps the turbulent re-separation and resulting expanding long bubble outboard as shown in the bottom left portion of Fig. 12.

For wings of moderate-to-high sweep these spanwise pressure gradients can be of sufficient magnitude to convert the expanding long bubble flow into a part-span, sometimes called Ram's Horn, vortex flow illustrated in Fig. 12. The mechanism sketched here is a notional model for *incipient vortex separation* from a smooth-edged wing. Section 4.0 discusses this model further in light of wind tunnel data and CFD simulations. See also the Visbal and Garmann [50] WRLES simulations when they add sweep to the wing. Küchemann [11] presents additional insights on swept-wing flow characteristics.

Stalling characteristics

Once formed, the vortex moves with increased incidence inboard along the trailing edge, grows stronger over the more forward stations and alters considerably the distribution of lift over the wing surface, and therefore the pitching moment also. Figure 12 bottom right shows the corresponding stall characteristics of a 48°-swept wing represented by section lift and moment diagram [47].

The presence of vortex flow produces *undesirable* pitching-moment characteristics. The *initial dip* in the pitching-moment curve occurs when the vortex has formed with appreciable strength over the outboard sections. As the vortex moves inboard with an increase in α, it leaves the tip sections in a diffused region of separated flow and their lift-curve slopes decrease. At the same time the inboard sections are experiencing an increase in lift-curve slope due to the vortex. The *net change* in span loading associated with these effects causes a nose-down pitching-moment variation through the moderate lift range.

When the lift reaches $C_L = 0.5$, the vortex has moved inboard sufficiently to cause a switch in the net balance, and hence the nose-down pitching-moment turns abruptly into a pitch-up instability [47], which continues up to stall. At maximum lift the flow is virtually disordered and unsteady, and the lift and moment values decrease.

In the remaining sections we investigate representative examples of wings and configurations in two classes of aircraft in Fig. 8. Slender delta wings are discussed in Section 4.0, including smooth-surface incipient vortex separation. Section 5.0 addresses not-so-slender delta and/or swept wings, including their stalling characteristics, and Section 6.0 presents the *tailoring* of early aircraft swept wing details to mitigate undesirable effects.

4.0 Slender delta wing aircraft

It is now common industrial practice to design wings using CFD and to confirm the results in the wind tunnel, so that very few wings are tested. CFD predicts flows in cruise conditions that are useful in engineering design [35, 51], as witness the progress demonstrated in the Drag Prediction workshops [52]. But outside the cruise range, separated flows are the norm, and there is less confidence in CFD. RANS computations with current turbulence models have been found unreliable at high lift and near-stall conditions. The impression is that physical model development for separated flows as well as for transition from laminar to turbulent flow has stalled and is a bottleneck to more widespread usage of CFD in aerodynamic design [35].

This section illustrates several aspects of this bottleneck involving vortex interactions over a slender aircraft. A unique flight-test program, initiated by NASA with subsequent collaborative assessment programs, focused on CFD prediction of the flight data.

4.1 F-16XL – a flying laboratory

In the 1990s, NASA conducted a flight-test program to study wing aerodynamics with a General Dynamics F-16XL aircraft. This slender aircraft has a highly swept inner wing panel, designed for efficient supersonic cruise, with a cranked leading edge such that the outer wing panel has substantially less sweep. This hybrid wing is not dissimilar to the J35, positioned far right in Fig. 8. The CAWAPI program focused on obtaining wing data over a broad range of operating conditions, as seen in Fig. 13.

https://doi.org/10.1017/aer.2023.39 Published online by Cambridge University Press

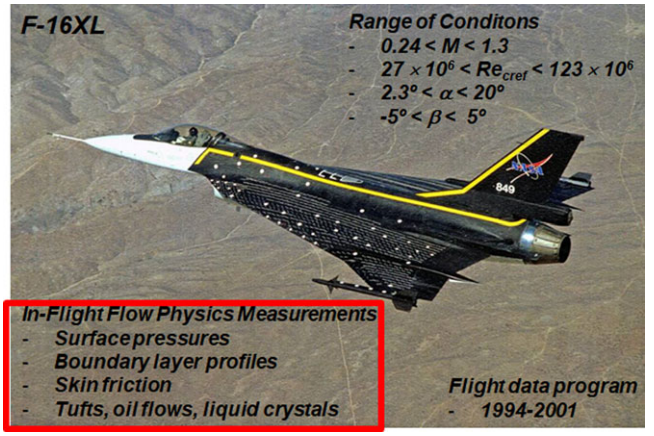

Figure 13. *The F-16XL Flying Laboratory with tables of flight conditions and measured data.*

NASA instrumented the F-16XL to provide a wealth of flight data, including pressure maps through the transonic speed range that provided a unique, but time-limited, opportunity for CFD correlation and code validation with flight and wind-tunnel data.

Although not explicitly discussed as such at the time, many of the difficulties in predicting the aerodynamics of the F-16XL stem from vortex interactions, including:

- Vortex-vortex interactions due to the cranked leading edge
- Vortex-shock interactions at the transonic and supersonic test conditions.
- Vortex-surface interactions due to the wing primary vortex inducing not only secondary vortices but also an additional vortex from the edge of the downstream wing component known as an *air dam*

A succession of three international programs was executed to seek improved CFD predictive capability of vortex flow aerodynamics at full-scale flight conditions. The first of these was CAWAPI and was performed as part of the RTO Task Group AVT-113. Luckring [2] discussed in detail the findings of these three programs. For our purposes the discussion here briefly summarises the current level of credibility in CFD predictions of vortex-separated flow over the F-16XL focusing on due-diligence investigations of numerical and physical modeling sensitivities.

Moderate interaction case – flight condition FC-7

Supercomputer capacity grew over the course of the CAWAPI investigations and enabled grid densities to increase an order of magnitude from 1.4 M cells to 15 M cells improving the numerical accuracy of the simulations. The differences in correlations among the various contributors to CAWAPI-1 were not very significant for the Flight Condition FC-7, ($M_\infty = 0.3, \alpha = 11.9°, Re_{cref} = 44.4 \times 10^6$) typical of low speed loiter. The wing flow exhibits, for the most part, moderate vortex-vortex interactions. Primary and secondary vortex systems are developed on both the inner and outer wing panels but remain far apart from each other. The secondary vortex under the inboard leading-edge vortex is obtained. The generally good correlations between simulations and flight data would suggest that the physical modeling used in RANS is sufficient for this category of vortex flow.

4.2 Low-speed landing condition FC-25

The CAWAPI work also identified two of the flight conditions that were not well predicted by all participants and warranted further investigation. These became the focus of the CAWAPI-2 effort. Discussed

https://doi.org/10.1017/aer.2023.39 Published online by Cambridge University Press

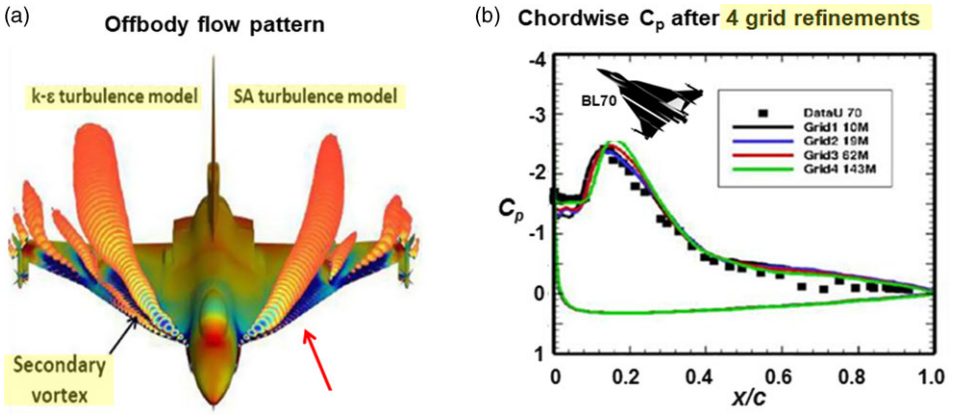

Figure 14. *Secondary vortex predictions by RANS, CAWAPI-2. FC-25: Elmiligui et al. [53]. (a) Vortex visualisation, and (b) chordwise pressure predictions, four different grid resolutions and flight data.*

here is the low-speed case with conditions FC-25, a subsonic high-alpha flow typical for approach in landing, $M_\infty = 0.24$, $\alpha = 19.8°$, $Re_{cref} = 32 \times 10^6$. The flowfield contains a much stronger vortex-vortex interaction on the outboard panel amongst the inboard leading-edge vortices, a counter-rotating air-dam vortex, and the outboard vortices, which standard physical modeling has more difficulty to predict accurately.

4.2.1 RANS simulation

Several possible sources for the discrepancies in FC-25 were identified. The observed sensitivities to grid resolution and turbulence modeling led to two additional assessment campaigns, CAWAPI-2 and CAWAPI-3.

One contribution from CAWAPI-2 was the due diligence that Elmiligui et al. [53] applied in obtaining their solution shown in Fig. 14 for FC-25. Secondary vortices form from smooth-surface separation, and through a combination of four levels of grid resolution and turbulence model assessments, Elmiligui et al. [53] achieved improved secondary vortex resolution with correspondingly improved correlations with the flight test data. In this case, the improved predictions came from the $k - \varepsilon$ turbulence model, while the Spalart-Allmaras (SA) model yielded no secondary vortex even after substantial grid refinement. The primary vortex sets up a significant adverse pressure gradient in the spanwise direction of the upper wing surface that causes the boundary layer to separate and form the secondary vortex. Near separation and in the presence of strong pressure gradients, the boundary layer is expected to be in non-equilibrium with production, transport and dissipation of turbulent kinetic energy changing rapidly and far from the state on which turbulence models are based. The two turbulence models in question show major differences in the treatment of turbulent kinetic energy. The two-equation $k - \varepsilon$ model solves for the transport of turbulent kinetic energy and its dissipation rate, while the one-equation SA model solves only for the transport of turbulent kinetic viscosity coefficient, substantially different from the energy transport equation in $k - \varepsilon$, suggesting that SA fails because it does not transport the right quantities.

Elmiligui et al.'s [53] findings demonstrated that difficulties remain for resolving separated vortex flows at differing scales with well-established turbulence models. The secondary vortex difficulties could relate to emergent shear-layer separation flow physics as is discussed below in the diamond wing studies.

The unsteady flow simulations from CAWAPI-2 indicated that more detailed unsteady work with finer grid resolution held out promise for simulating the FC-25 case, and it became the focus for the CAWAPI-3 investigations with hybrid RANS-LES modeling.

https://doi.org/10.1017/aer.2023.39 Published online by Cambridge University Press

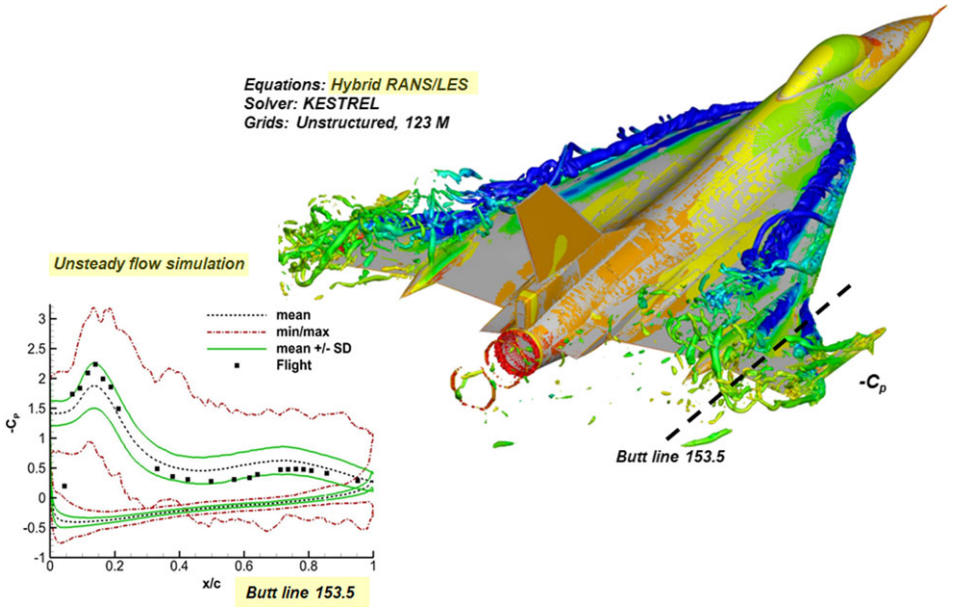

Figure 15. *CAWAPI-3 Hybrid RANS/LES simulations, FC-25. Right, vortex visualisation [54]; left, butt line 153.5 computed time mean and variation pressure profiles and flight data [55].*

4.2.2 Hybrid RANS/LES simulation

One of the major findings of the CAWAPI-2 work, summarised by Rizzi and Luckring [35], is that unsteady flow, possibly with the vortex breaking down over the outer wing panel, occurred in FC-25. The CAWAPI-3 Assessment studied this question further with hybrid RANS/LES simulations [2], and Fig. 15 summarises one set of the results of Morton and McDaniel [54].

Comparisons among the methods of the overall vortical flows were quite good. The hybrid RANS/LES simulations brought out detailed vortical content and substructure, including stronger secondary vortices than often observed with RANS. Exact causes for this are difficult to pinpoint, but could include finer/adapted grids, and the inherent modeling capabilities of the LES resolution of vortical scales over the wing. Presenting vorticity colored by the pressure coefficient, Fig. 15 exemplifies the solution of Morton and McDaniel [54] obtained on a grid of 123 M cells adapted in both space and time.

The primary vortex (dark blue) from the inner (70° sweep) wing appears to burst before the trailing edge, and the secondary vortex (lighter blue), slightly outboard of the primary, seems to merge with the dark-blue air-dam vortex (both are counterrotating). Another leading-edge vortex (dark blue) forms over the outer (50° sweep) wing panel, and further outboard, this vortex merges with several smaller vortical structures from the tip missile, all of which break down before the trailing edge. The vortex breakdown mechanism creates turbulent kinetic energy that must be modeled properly or be resolved. Many turbulence models create orders of magnitude too much turbulent eddy viscosity in the primary vortex core, which significantly alters the flowfield, and in some cases, eliminates the breakdown observed experimentally at high Reynolds numbers.

Chordwise pressure correlation

The plot of the computed pressure distribution along Butt Line 153.5 in Fig. 15, from Lofthouse and Cummings [55], indicates the complexity of the vortex interactions taking place over the wing outer panel. Plotted are the: (i) mean, (ii) maximum and minimum, and (iii) mean plus/minus one standard deviation, values of the computed unsteady surface pressure. The flight-test data shown are steady, a sort

https://doi.org/10.1017/aer.2023.39 Published online by Cambridge University Press

of time-average obtained with the steady-flow sensor technology used, that correlate not unreasonably with the mean computed pressure, and fall within the standard-deviation band.

Overall one concludes that hybrid RANS-LES modeling represents better than RANS the aerodynamics over the outer wing panel with interacting vortices at this condition. A summary of the CAWAPI-3 findings was published in 2017 in a special section of the AIAA *Journal of Aircraft* with an introduction by Luckring [56], see also Luckring [2].

4.3 Vortex breakdown: unit-problem study

The discussion of the vortex-flow aerodynamics in Figs. 14 and 15 highlighted two mechanisms that require further study, namely *vortex breakdown* and the *incipient vortex* lifting-off from a smooth surface. This section studies these two phenomena as *unit problems*.

Delta-wing vortex breakdown has been studied extensively since the 1950s. Despite the lack today of a universally accepted unified theoretical interpretation, several forms of vortex breakdown have been identified experimentally, namely bubble and helical types, and the global characteristics of the phenomena are understood.

The consequences on flight performance are great if the vortex bursts over the wing because then the time and space scales grow, the flow fluctuates, the separation becomes extensive, and lift decreases. It can be one source of wing buffet and pitch-up instability.

The core of a vortex breaks down when, at some point along its axis, the strong regular spiral motion suddenly becomes weaker and chaotic, as Fig. 16 indicates. In breakdown, the mean axial velocity component on the vortex axis rapidly decreases until it reaches a stagnation point and/or reverses.

This stagnation point, called the breakdown location, is unsteady and typically oscillates about some mean position along the axis of the vortex core. As angle-of-attack is increased, the mean vortex breakdown location moves upstream over the delta wing from the trailing edge toward the apex. The vortex bursts above the wing when the adverse pressure gradient occurring at the trailing edge becomes sufficiently large.

Contributions to understanding the mechanisms of vortex breakdown were achieved experimentally and numerically through the STO project AVT-080 [59]. Although hybrid RANS/LES technology has improved the physical modeling, high-confidence predictions have yet to be demonstrated.

The water-tunnel experiments of Lambourne and Bryer [57] in Fig. 16 reveal the two basic types of vortex breakdown over a sharp-edged delta wing: the axisymmetric bubble-type and the non-axisymmetric helical (spiral) type.

In the spiral type of breakdown the core flow decelerates rapidly. Immediately downstream, the vortex core filament abruptly kinks and starts to spiral around the axis of the structure, forming a corkscrew-like distortion of the vortex core (see sketch in Fig. 16). The spiral structure can persist for one or two turns before breaking up into large-scale turbulence.

From computations carried out by Görtz [58], Fig. 16 presents an iso-surface of total pressure, coloured in magnitude of axial velocity along the core, also visualised is the feeding shear layer issuing from the sharp leading edge. The time sequence of computed images in Fig. 16 shows the evolution from spiral to intermittent bubble-type breakdown at $\alpha = 30°$.

Time advances from top to bottom. At the first instant in time, top, the port and starboard iso-surfaces form symmetric cork-screw-like distortions winding in the direction opposite to that of the upstream vortex. At the later instance, bottom, bubble-type breakdown is established over the port-side of the wing with spiral-type breakdown occurring simultaneously over the starboard side. This transformation always occurred in a transient sense for short periods of time and was associated with a significant upstream movement of the breakdown location. The bubble transformed back into a spiral after some time to reappear as a bubble again at a later time on the opposite side of the wing (not shown here). Such intermittent bubble-type breakdown was also predicted in time-accurate CFD simulations of the flow around a 65° stationary delta wing at $\alpha = 30°$ by Gordnier [60].

https://doi.org/10.1017/aer.2023.39 Published online by Cambridge University Press

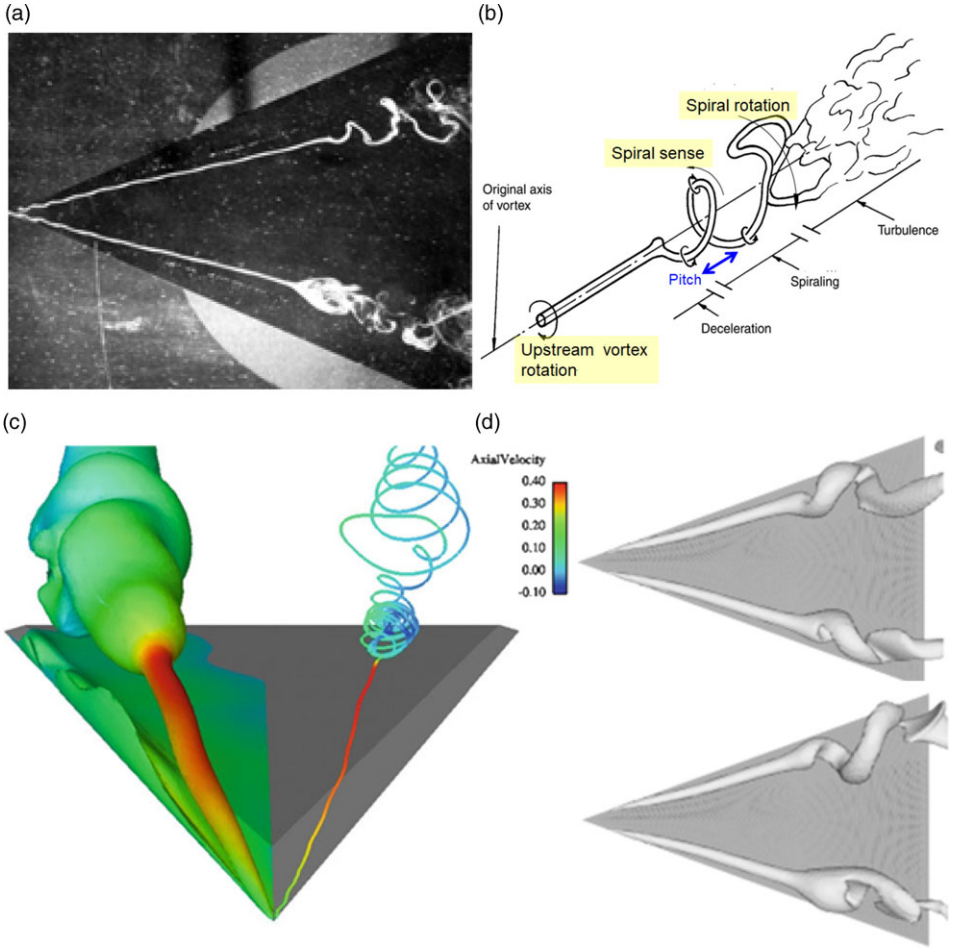

Figure 16. *Vortex dynamics of spiral-type vortex breakdown. (a) Water tunnel experiment showing spiral and bubble type breakdown [57]; (b) sketch indicating the main dynamics of spiral vortex breakdown [57]; (c) computed total pressure iso-surface and vortex core filament [58]; (d) time sequence of images showing the evolution from spiral to intermittent bubble-type breakdown [58], iso-surface of entropy.*

CFD simulations today resolve many of the characteristics of vortex breakdown, but the uncertainty in the physical modeling of the burst turbulent core remains substantial. Scale-resolved LES computations could provide further insight into the flow physics that is involved. Perhaps even a DNS computation of the Lambourne and Bryer water tunnel experiment might be possible since the Reynolds number is very low 16×10^3 and the edge is sharp.

4.4 Smooth-surface separation: unit-problem study

Practical wings have rounded, i.e. blunt, leading edges, and one difficulty for CFD to simulate accurately is the formation or onset of the blunt-leading-edge vortex. A sharp-edged wing geometrically fixes the separation location to the leading edge, and the requirements for RANS to work well are fulfilled. However, when the wing surface is smooth, the location where the turbulent shear layer leaves the surface sees a balance of the inertial and viscous forces in the Navier-Stokes equations that can be sensitive to the turbulence modeling as well as the surface and near-wall grids.

https://doi.org/10.1017/aer.2023.39 Published online by Cambridge University Press

We have seen above in Figs. 14 and 15 examples of sensitivity in the modeling of the secondary vortex forming over a smooth surface and of the primary vortex forming on the blunt leading edge of the outer panel of the F-16XL with sweep 50°. This moderate sweep, similar to the wings of current UCAVs, is known to make accurate simulation of the incipient separation difficult. But this is not a new problem. It presented itself already in the design of the first-generation swept-wing fighters in the late 1940s. It motivated the Polhamus phenomenological model of incipient vortex separation discussed in Section 3.2.1 and displayed in Fig. 12. In a comprehensive wind-tunnel campaign, Poll [61] studied the formation and development of spiral vortex flow over swept-back wings of varying sweep angle and leading-edge radius. From what he learned in the wind tunnel, Poll proposed mechanisms for the formation of spiral vortices from the various blunt leading edges.

Not taking account of Poll's work on arrow wings, the NATO Task Group AVT-183 [62] set up a program to study blunt-leading-edge vortex separation as a unit problem. This work focused on a 53° swept diamond wing with a blunt leading edge in a manner relevant to challenges discovered on a UCAV configuration of interest to another NATO Task Group, AVT-161 [63].

4.4.1 Origin of vortex: WT & CFD studies

The origin of the leading-edge vortex affects its strength and location over the wing, which makes it a critical feature to the credibility of a CFD simulation.

This section summarises two studies of incipient vortex separation: Poll's wind-tunnel investigations [61] and the AVT-183 CFD computations [62]. Although these two studies are totally unconnected in time and the geometries are different, the overall flow patterns are remarkably similar and correlate nicely with the Polhamus phenomenological model for the origin of the leading-edge vortex.

On the left, Fig. 17 presents oil-flow over the 45°-swept wind-tunnel model at $\alpha = 16°$. Poll [61] carried out an alpha sweep for this wing starting from zero. A short leading-edge bubble formed at the tip at 4° incidence. Increasing the incidence caused the upstream end of the bubble to move closer to the root where it re-attaches, while outboard it only re-attaches near the trailing edge, thus forming a long separation bubble, or else fails to attach and rolls up to form a strong vortex very close to the wing. Beyond 9° incidence the vortex bursts over the wing, causing the attachment line to terminate part way across the span while a blob of oil is entrained on the leading edge at approximately the same spanwise location as the vortex burst.

As the incidence was increased further to 12°, the part-span vortex origin moved along the leading edge towards the root, as did the oil-blob eye, and a line of secondary separation developed as shown in Fig. 17. In a similar wind-tunnel study, Black [65] observed much the same flow patterns as Poll.

On the right Fig. 17 conveys the global features of the diamond wing flow field at $\alpha = 12°$ through the visualisation of the computed off-body and surface flow data of Frink et al. [64]. The vortex core (thick black line) emerges from the incipient separation region midway along the blunt leading edge and continues downstream over the outer portion of the wing. Near the trailing edge, the vortex core displays some instability, which along with the associated diffusion of the reattachment line may indicate vortex breakdown. A second clustering of converging streamtraces is observed (Fig. 18) in the predominantly attached flow region of the wing where an inner vortex is forming, which may be unique to the diamond planform since no such vortex was identified by Poll [61] or Black [65]. The incipient separation region bears some resemblance to Poll's flow patterns and is discussed next.

Features of incipient separation region

On the right Fig. 18 looks more closely into the region of incipient separation that culminates with the formation of a part-span leading-edge vortex, as seen in Fig. 17.

The beginning of incipient separation in Fig. 18 is defined by a set of dividing streamtraces that cross the leading edge at $x/c_R = 0.166$, z=0 where the balance between streamwise inertia and spanwise pressure gradients is tipped. All leading-edge boundary-layer flow downstream of $x/c_R = 0.166$ is contained outboard of these dividing stream-traces and eventually returns to the leading edge, as in the

https://doi.org/10.1017/aer.2023.39 Published online by Cambridge University Press

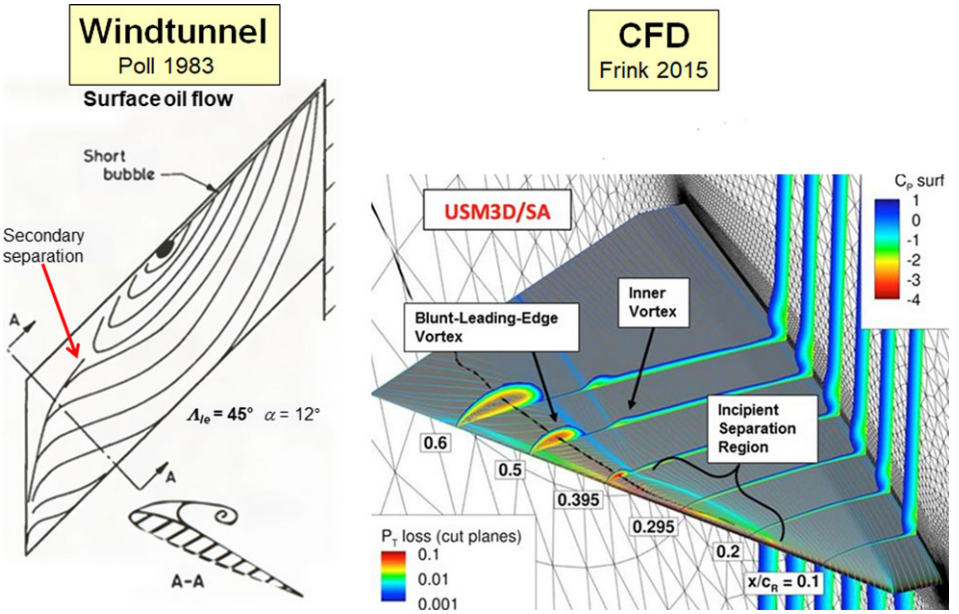

Figure 17. *Blunt-edge vortex separation, experiment and CFD. Left, WT oilflow interpretation as surface flow, Poll [61], 1983. Right, 53° diamond wing at* $M_\infty = 0.15, Re = 2.7 \cdot 10^6, \alpha = 12°$*, total pressure loss in cuts and vortex core trace, Frink et al. [64], 2015.*

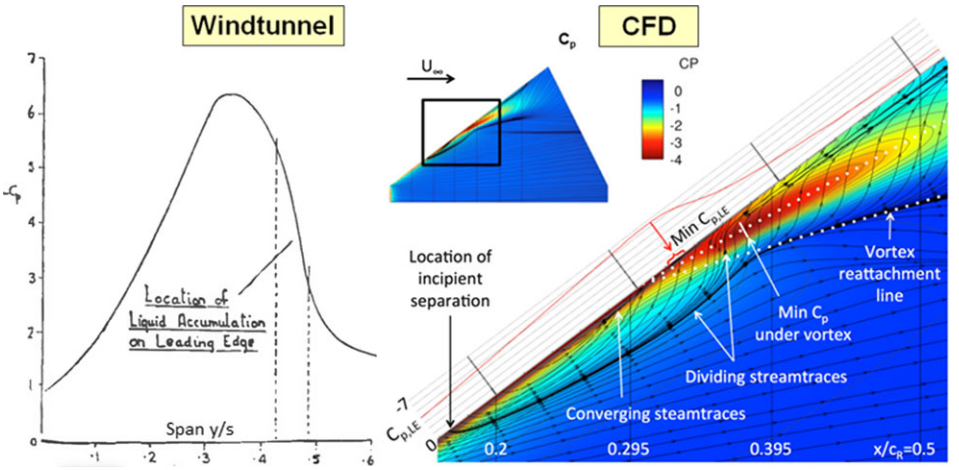

Figure 18. *Features of incipient separation regions, experiment and CFD. Left,* C_p *in WT at leading edge, (Black [65], 1956). Right, CFD, same case as Figure 17, surface streamlines and* C_p*,* C_p *graphed at leading edge [64], 2015.*

short bubble in Fig. 17. All streamtraces upstream of $x/c_R = 0.166$ continue across the predominantly attached-flow upper surface and exit at the trailing edge, as in a long bubble that either re-attaches or not.

The plot of Cp_{LE} versus span along the leading edge reveals an unusually high suction level with a minimum value nearly -7. Similar suctions values were in fact measured in wind-tunnel tests by Black [65], as plotted on the left in Fig. 18. Poll [61] and Black [65] both associated high suction with the

https://doi.org/10.1017/aer.2023.39 Published online by Cambridge University Press

oil blob eye they observed. The deep suction trough, colored red in Fig. 18, might well entrain oil in an oil-flow study. Frink et al. [64] argue that the minimum pressure location is at, or very near to, the theoretical start of the primary vortex on the blunt leading edge. The broad similarities in flow patterns seen in these experiments and the CFD simulation support the notion suggested in Fig. 12 how a short separation bubble followed by a long bubble of turbulent re-separation in the presence of spanwise flow due to sweep could well be a mechanism for incipient vortex separation. This means that processes such as transition, entrainment etc., which take place in the free shear-layer immediately downstream of the primary separation line are affected by free-stream turbulence levels and turbulence spectra, making CFD simulations sensitive to its physical modeling.

5.0 Not-so-slender swept-wing aircraft – UCAVS

Typical UCAV configurations have not-so-slender wings with moderate leading-edge sweep angles of 45° to 60°, and place in the centre of Fig. 8. Planforms vary from pure Δ to ◇ and even λ more or less blended wing bodies with a relatively small thickness ratio at the inner wing/fuselage region. The performance and low-observable signature considerations require a compromise between a small radar cross-section and lifting surface shapes for long range and sufficient agility. The airflow is governed largely by the progression of vortices shed from the wing leading edge which interact and produce non-linear aerodynamics. UCAVs may exhibit undesirable flying characteristics over part of the envelope due to tip stall and pitch-up. Such problems on early swept wing fighters, e.g. the Saab J32 discussed in Section 6.0, were mitigated by vortex control devices like leading-edge fences and notches which would violate the low observable requirement.

The design of UCAV wings continues to be a major research and development activity. Missions require efficient high-speed flight, loiter and good stability and handling at low speeds for good landing qualities. Figure 19 shows the X45A, X47A, and SACCON. The NATO-RTO AVT-161 Task Group [66] was a comprehensive research program designed to investigate the ability of computational methods to predict stability and control characteristics of a generic unmanned combat air vehicle, (SACCON).

The SACCON tailless, λ-shaped flying wing configuration is a UCAV concept with a 53° swept wing with parallel edges for low radar signature, defined as a benchmark for CFD methods and wind-tunnel experiments.

5.1 Analysis of UCAV stalling characteristics

The SACCON exhibits adverse aerodynamics at low speed and high lift that results in poor stalling characteristics, evidenced in the C_m versus α curve[3]. The subsonic $M_\infty = 0.5$ case with mild compressibility effects illustrates in Fig. 20 the different flow regimes as the angle-of-attack is increased. At low angles of attack, the pitching moment changes linearly with α, with attached flow over the wing, persisting until around $\alpha = 10°$ where the C_m curve bends slightly upwards. As the angle-of-attack increases to 14°, the C_m curve turns sharply downwards – the start of the kink in the pitch moment – only to swing up again around 16° or 17°. Although these RANS computations of C_m do not exactly match those of the wind-tunnel measurements, they provide useful information about the nonlinear behaviour of the aircraft. But such agreement unfortunately is not consistent across conditions and cases, so much experience is needed to ascertain the validity of a specific case. For example, at lower speed the agreement in C_m is worse, a case in point that the reliability of RANS predictions in the nonlinear regions of the flight envelope is questionable.

Three flowfield visualisations in Fig. 20, at $\alpha = 14°$, 17° and 19°, illustrate the vortex patterns responsible for the kink that evolves with increasing α. Shown are streamlines seeded to identify the vortices, while contours of C_p over the upper surface indicate the pressure field. The flow pattern is dominated by the movement and interaction of two leading-edge vortices. At 14° the visualisation suggests that a

[3]The M-Edge code results are from Eliasson et al. [67], the other CFD and WT results are from Coppin et al. [68]

https://doi.org/10.1017/aer.2023.39 Published online by Cambridge University Press

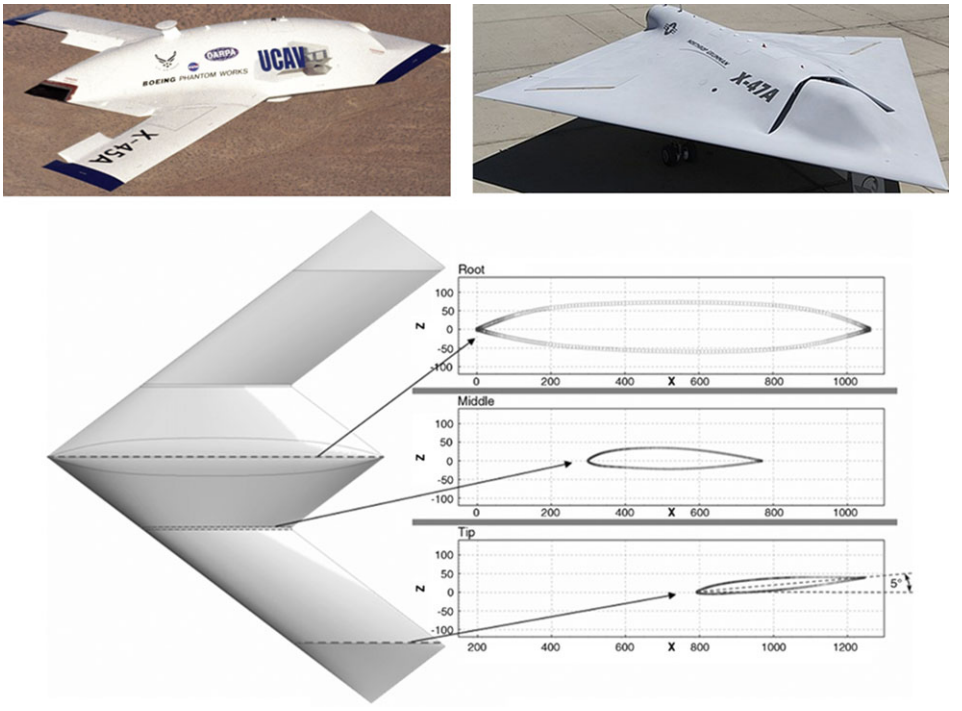

Figure 19. *UCAV examples. Top: X-45A and X-47A; bottom: SACCON main geometry.*

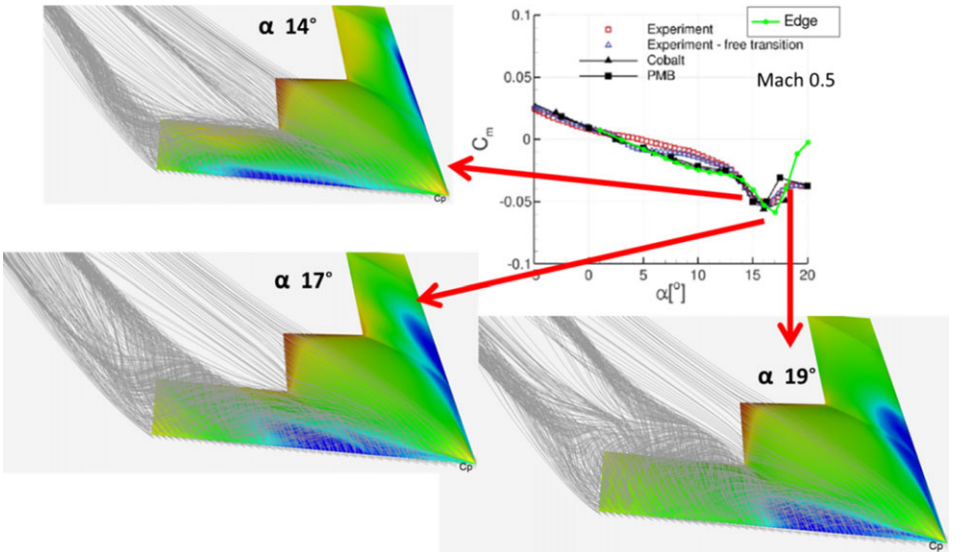

Figure 20. *Flow visualisation for the clean SACCON configuration;* $M_\infty = 0.5$. *Left: streamlines over surface* C_p *contours [67]. Top right: pitching moment curve, CFD and WT results [67, 68].*

https://doi.org/10.1017/aer.2023.39 Published online by Cambridge University Press

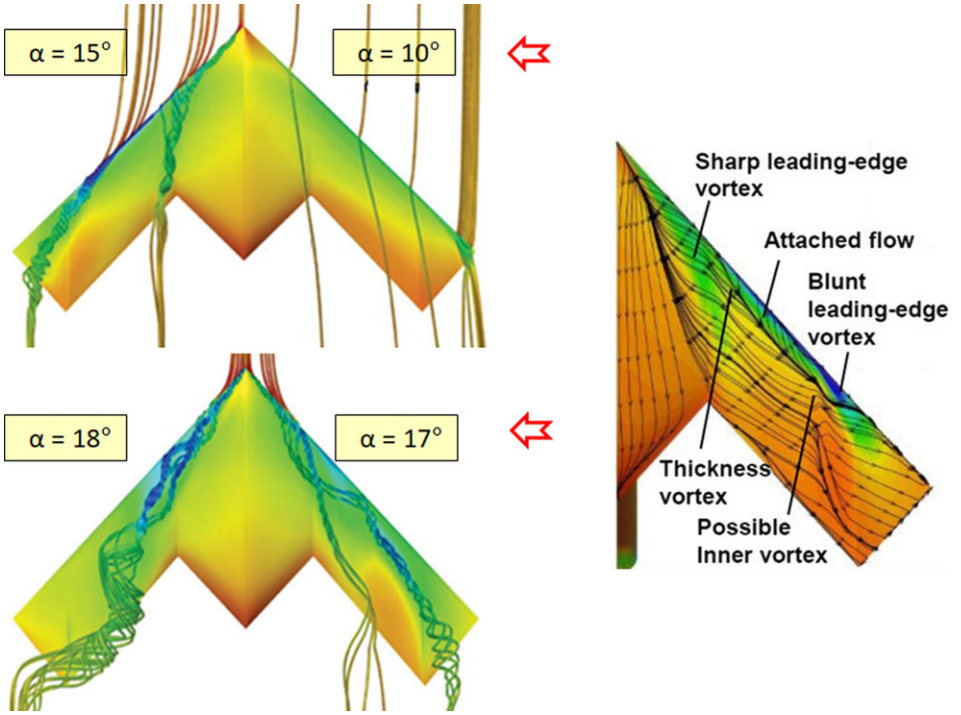

Figure 21. *SACCON interacting vortices. Left, from attached flow to vortex merging with loss of local lift [68]. Right, vortex system* C_p *footprint and skin friction lines [70].*

part-span (Ram's Horn) vortex starts somewhat outboard of the apex, aligned with the leading edge until it turns downstream a little before the tip. At 17°, the minimum of the kink, the downstream turn in the Ram's Horn vortex travels inboard, while a second vortex is shed from the apex to interact with it. At 19°, the C_m curve has turned sharply upward indicating pitch-up instability. The two vortices just outboard of the apex appear to have merged, suggested by the streamlines spiraling downstream of the low-pressure footprint in the isobars. Outboard of this region is chaotic vortical flow, presumably vortex breakdown with loss of suction, indicative of stall, occurring over the ailerons with dubious control authority. This interaction moves forward with increasing angle-of-attack, causing an increasing pitching moment, seen in the C_m-curve, strikingly similar with the C_m (C_L) curve in Fig. 12 bottom right.

5.2 Dynamics of interacting vortices

A similar flow topology is seen at lower Mach numbers, i.e. $M_\infty = 0.146$, with the forward motion of the tip vortex and the vortex breakdown occurring at lower angles of attack as the Mach number is reduced. Coppin [68] has visualised the vortex dynamics for this case shown in Fig. 21. The description here follows that of Coppin [68] and Schütte [69]. Similar to the case in Fig. 20, attached flow over the wing persists until around 10° angle-of-attack (Fig. 21 top), when a vortex forms at the wing tip, where the wing profile is sharp. As the angle-of-attack increases to 15°, an apex vortex has formed, which tracks the sharp leading edge and then moves inboard. Meanwhile, the tip vortex onset location continues to move forward. The onset of the tip vortex has reached the section on the wing where the profile is blunt. Figure 21 right shows the skin friction lines reported by Hövelmann [70] at 15° indicating the surface details of these interacting vortices.

The motion of the tip vortex continues forward with increasing angle-of-attack, illustrated in Fig. 21 bottom left, 17°, until there is no attached flow between the apex vortex and the tip vortex. Then, the

https://doi.org/10.1017/aer.2023.39 Published online by Cambridge University Press

apex and tip vortices interact, and this combined region of vortical flow has a vortex breakdown location that moves forward with increasing angle-of-attack.

The flow pattern for all sub-critical Mach numbers therefore consists of two vortices, whose onset locations change in a nonlinear fashion with the angle-of-attack and which eventually interact and breakdown.

6.0 Tailoring Swept-Wing design – J29 and J32

In the same spirit that Lanchester assessed the designs of the Wright and Voisin flyers, discussed in Section 2.0, this section investigates several design features of the two swept-wing Saab fighters, the J29 and J32.

We have seen that wing sweep brings lower wave drag, but slender swept wings also are prone to tip stall accompanied by pitch-up. The stall characteristics deteriorate with increased wing sweep. So how does the wing designer reach a workable solution to give the aircraft acceptable flying qualities? Chief aerodynamicist at Douglas Aircraft, A.M.O. Smith, characterised an airplane to be a 'device that almost won't work', by which he meant that to achieve the highest performance you are always pushing up against the boundaries of what is just possible. Another aerodynamicist, George Schairer at Boeing Aircraft, stated that 'applying sweepback to aircraft required extensive development of new concepts for many design details, needing special and different *tailoring of details*'. What tasks face the designer in carrying out such tailoring? Let us answer this question in the context of swept-wing design.

Designing a wing involves a number of basic actions, exemplified here by the design of high-speed aircraft

- *Exploit* a concept offering some benefit in performance: in our example, sweep the wing to reduce wave drag.
- *Tolerate* unwanted consequences: Wing sweep gives lower lift and makes the tip prone to stall with possible pitch-up instability.
- *Mitigate* the negative effects: for example, by flow control devices.

The design must ensure, as far as is practical, *controlled flight* across the flight envelope, the most fundamental flying quality. The swept-wing design must encompass means to maintain control surface authority to check uncommanded nose-up pitching, wing drop or roll. The Me-262 pioneered automatic leading-edge slats to keep flow over the outer wing attached, and Sections 6.1 and 6.2 describe devices adopted on the Saab J29 and J32.

However, should the airplane fly out of control, *means of recovery* must be provided. The J29 has stability problems on approach with landing flaps. The test pilots warned about 'crossed controls' with ailerons and rudder. Still, inexperienced pilots had problems, and a significant number of fatal crashes was suffered. The problem was successfully addressed by pilot training. First, train to avoid crossed controls; second, to use smaller flap deflection at landing; and third, to use rudder rather than ailerons for yaw and roll control.

Forensic CFD

To make these considerations more concrete look at what the Saab aerodynamicists did to realise the J29 and J32. The most direct way would be to read how they went about designing the wings for these two aircraft. Most airplane designers, however, have not left behind any detailed accounts of how they made their choices, either verbal or written documents. Moreover, asking different people working on the same airplane project may give conflicting accounts of the reasons for its features, each to their own pet theory.

Another dead end is that such information is company confidential, and the aerodynamicist is not allowed to explain what he or she did. The end result, all so often, is that we must *guess* why wings, and entire airplanes, are shaped the way they are. There is, however, one way forward, namely re-study the

https://doi.org/10.1017/aer.2023.39 Published online by Cambridge University Press

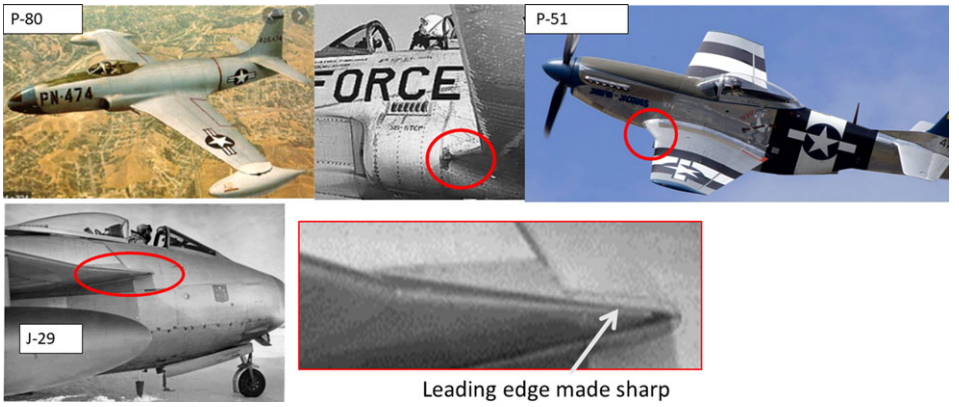

Figure 22. *Leading-edge extensions, small on the P-51 and P-80, substantial on the Saab J29.*

problem today with CFD in a procedure we call *forensic CFD*. That allows us to derive a cause-effect argument about design choices taken. For example, you can make two simulations, one with a wing fence and the other without the fence. Comparing the two results shows what effect the fence has on the flowfield and the aerodynamic forces[4].

6.1 J29 CFD case study

The following presents details for the Saab J29 Tunnan with 25° sweep (1948) and the J32 Lansen (1952) with 35° swept wing. A complementary story of the J29, in particular the design modification on the E model with a small fence and a sawtooth on the leading edge, is given in the textbook [9]. The discussion here focuses on the J29 leading-edge root extension and the effect of the mini leading-edge fence on the J32. The J32 wing planform is similar to those of its generation comrades (F-86, MiG-15), Fig. 11 left, and to outer wings on UCAVs, treated in some detail above. Vortex separation from the leading edge is stronger on the J32 than on the milder sweep of the J29, and the pitch-up is stronger, as shown in the stability diagram, Fig. 11 right, in the inset moment curves.

The F-86 and Saab J32 are on the instability side of the neutral zone (cross-hatched) whereas the J29 is on the stability side. The flow physics responsible for the behaviour is illustrated in Fig. 12. The distinction made there is on the type of separation correlated with leading edge radius and sweep. We see that Saab engineers stayed safe with their first swept wing: the J29 is more on the benign side with trailing edge separation, and the J32 more on the leading edge separation side. The two points for each wing on the vertical axis indicate leading edge radius evaluated streamwise or normal to leading edge. We continue with an analysis of the J29 leading edge root extension (LERX) and return to a discussion of Fig. 12 in the analysis of the J32.

The Saab J29 had from the start a significant leading-edge extension with *sharp* leading edge. As Fig. 22 shows, smaller LERX appear both on the P-80 and the P-51. Speculations about the Me P1101 influence on the design of the J29 are ubiquitous. The first Me P1101 proposal from July 1944 had a large LERX, similar to the Saab J29, but was still significantly different with air intakes in wing roots. Later proposals lost the LERX and the wing root intakes, which were replaced by a nose intake.

6.1.1 LERX on J29 wing

As mentioned above, we must guess why wings are shaped as they are, and forensic CFD can help by detailing the flow physics of different design details. Let us explore this approach on the question of

[4]*All of the forensic CFD computations presented in this paper have been carried out with the M-Edge code.*

https://doi.org/10.1017/aer.2023.39 Published online by Cambridge University Press

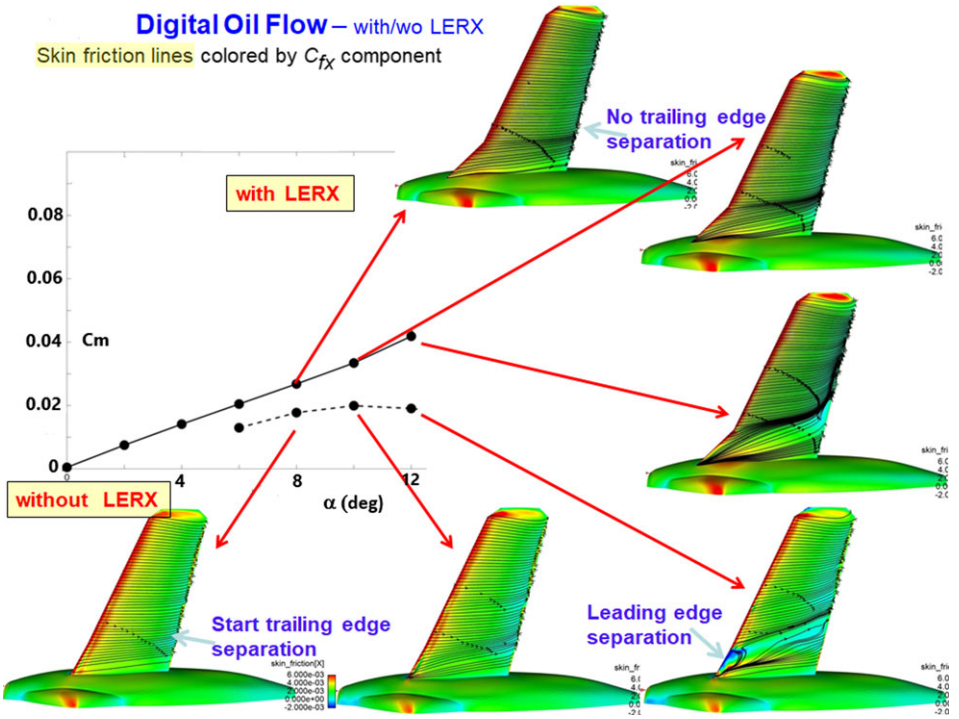

Figure 23. *Saab J29A wing body and imagined version without LERX. Moment curves, and skin friction lines, surface colored by x-component of skin-friction force vector.*

the LERX on the J29. Of the three first generation swept wing fighters, the J29 is the only one without a straight-line leading edge. The CFD was made on a parametric surface model created from paper drawings courteously lent to us by the Saab Veteran's Club. Models with and without LERX were analysed in different speed regimes.

Effect of LERX on leading edge separations

The potential effect on boundary layer flow, and hence tendencies to tip stall, were investigated by comparisons of the J29A wing-body with a version without LERX. The α-sweep results are shown in Fig. 23. The boundary-layer flow is visualised by skin-friction lines on the surface coloured by x-component of skin-friction force coefficient. The inset low-speed moment curves show how the LERX mitigates the non-linear progression. Note that the model has no tail, so the moment shown here is not representative for the full configuration.

The flow-physics interpretation is as follows. Consider the incidence progression $8^\circ - 12^\circ$ on the no-LERX wing. The trailing-edge separation is weak at 8° but obvious, as indicated for 20% semi-span at 10°. At 12° the separation has dramatically changed into a free vortex separating close to the fuselage. The net effect on flight mechanics is a curving of the moment curve.

The LERX wing has indications of a vortical separation from the leading-edge kink growing in strength with incidence. At 12° there is trailing-edge separation downstream of the kink, following from the increased lift-off of the vortex. The skin-friction footprint of the vortex separated at the kink, as interpreted above, is seen also in Fig. 24, keeping the flaps out of massively separated flow. Another beneficial effect of the LERX is that it draws the isobars forward to increase their sweep close to the fuselage. This decreases the transonic wave drag since the shock angle deviates more from normal.

https://doi.org/10.1017/aer.2023.39 Published online by Cambridge University Press

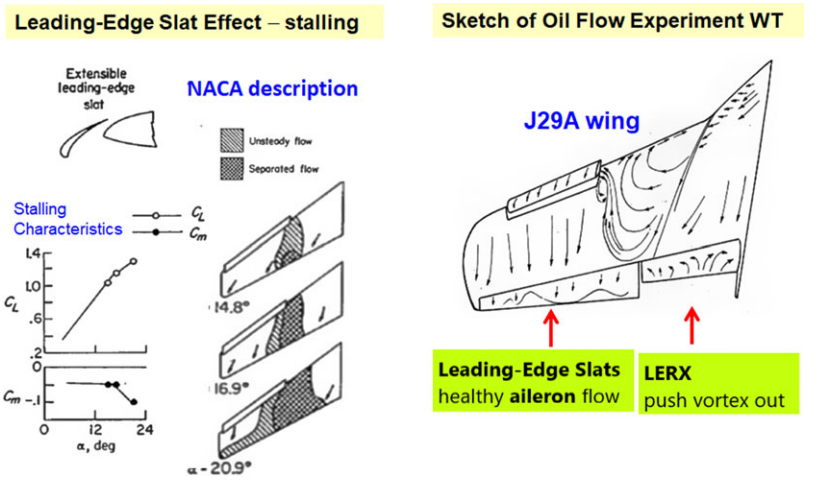

Figure 24. *Effect of leading-edge slat and LERX. Left: leading-edge slat effect on separation and moment curve [71]. Right: interpretation of boundary-layer flow from oil-flow visualisation in wind tunnel [72].*

6.1.2 How J29A wing preserves control authority

The J29A model has leading-edge slats on the outer wing, much like the Me 262 and the F-86. The combination of LERX and slats was effective in preserving the efficiency of ailerons and trailing-edge flaps. Taken from Furlong and McHugh [71], the slat effect is sketched on the left in Fig. 24, showing how the outer-wing flow is kept attached.

Interpretations of low-speed oil flow in wind-tunnel experiments [72] at FFA for the J29 are given to the right in Fig. 24. The accompanying text explains that while the arrows do show reverse boundary-layer flow, the LERX vortex, starting at the kink outboard, keeps the flow attached and stable. One could think of the interconnected effect of slats and LERX being that of establishing a large, but stable, recirculation bubble or vortex swirl between the root and the leading-edge slats.

6.2 J32 CFD case study

The Saab J32, with maiden flight 1952, was a transonic fighter developed to replace the J29, shown in Fig. 25. It has a simple linearly lofted wing with sweep 35° to give higher speed than the J29. Although it was originally conceived as an air-superiority fighter, it was soon realised that the speeds of new Soviet bombers made its speed performance insufficient for that role. With the Mach 2 capable fighter Saab J35 already sufficiently along in development to fly three years later, the J32 was re-cast to execute ground attack, reconnaissance, electronic countermeasures and jamming tasks.

6.2.1 J32 Fence mitigates pitch-up problem

The stall problems ubiquitous for swept wings are created by the movement of the leading-edge vortices as incidence increases. A similar leading-edge vortex phenomenon occurs on the Saab J32, as on the SACCON described above.

The phenomenological sketch in Fig. 12 of the physics occurring on leading-edge vortex formation tracks well the development with increasing angle-of-attack of the vortex over the Saab J32, as seen in Fig. 25. The initial leading-edge separation bubble becomes a spiral by the spanwise flow. At higher α the vortex lifts off and swings aft, forming a Ram's Horn vortex, leaving the tip in separated flow.

https://doi.org/10.1017/aer.2023.39 Published online by Cambridge University Press

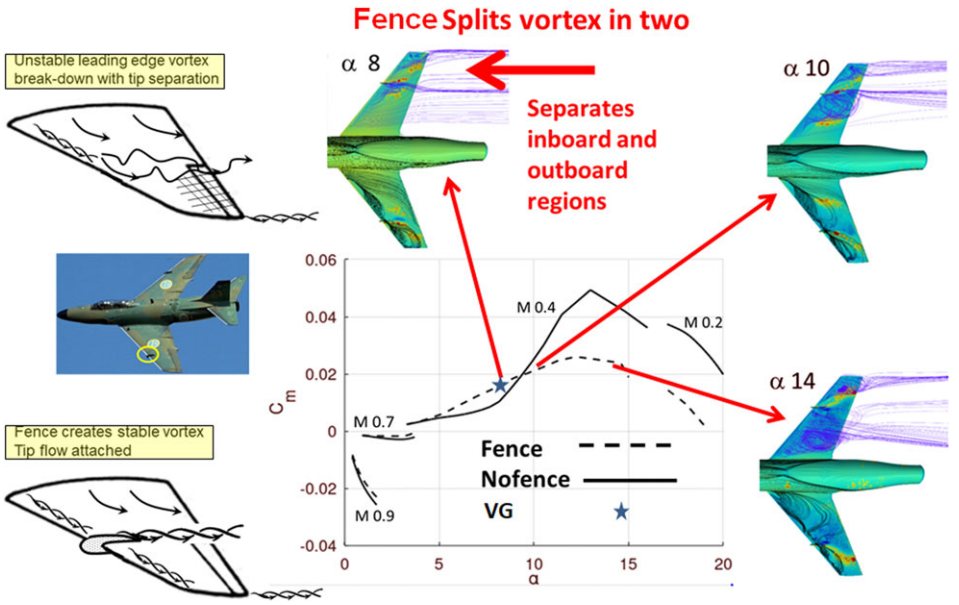

Figure 25. *Wing fence effects on stalling characteristics. Left: the fence splits vortex in two. Inset: moment curves with and without fence for several Mach values at sea level. Flow visualisations at selected α show stream lines and pressure coefficient over the upper (starboard) wings, x-component of skin friction and skin-friction lines over the lower (port) wings.*

After much flight testing, various alleviating measures were devised to delay separation or at least make it predictable. The Me262 and F-86 used leading-edge slats over much of the leading edge, with automatic or manual deployment at high angles of attack. Other most common minor measures are vortex-control devices, namely stall fences, seen on the MiG 15, leading-edge notches, saw-teeth, seen on Saab J29, J37, and J39, leading-edge chord root extensions LERX, and rows of small vortex generators as on the B-47 [17].

Most of these work by producing vortices that interact with the vortical flow over the clean wing to improve its characteristics. The function of the leading-edge fence is interpreted in Fig. 25, top and bottom, left. But the precise functioning of these devices is not easily predicted and must be studied by computation or experiment in each specific case.

The poor stalling characteristics of the Saab J32 wing were initially addressed by leading-edge slats test flown on a subscale wing. Further tests showed that a stall fence, called a vortex splitter by Saab engineers, properly placed on the wing was a simpler cure. Figure 25, middle, displays the moment curves for the angles of attack ranges reasonable for flight at $M_\infty = 0.2, 0.4, 0.7, 0.9$. Streamlines with surface C_p show the development of the vortices and their pressure footprints on the upper (starboard) wing semispans. Lower (port) wing semispans show skin-friction lines and surface coloured by $C_{f,x}$, blue for upstream skin-friction force, indicative of reverse flow. The fence clearly reduces the moment variation over the angle-of-attack range.

Fences like these are *un-stealthy*, so not applicable to modern combat vehicles. In a what-if CFD experiment, the fence is replaced in the computation by a pair of small converging vortex generators, to cause the vortex to lift off at the fence position. Their effect ought to be noticeable, on a par with that of the fence. In fact we carried out exactly this what-if CFD experiment on the SACCON [67], including variation of the vortex-generator (VG) positions to find their best effect. The finding was that indeed vortex generators can create an effect similar to the fence. See the star symbol in Fig. 25; a computation of the J32 with VGs instead of the fence confirms this.

https://doi.org/10.1017/aer.2023.39 Published online by Cambridge University Press

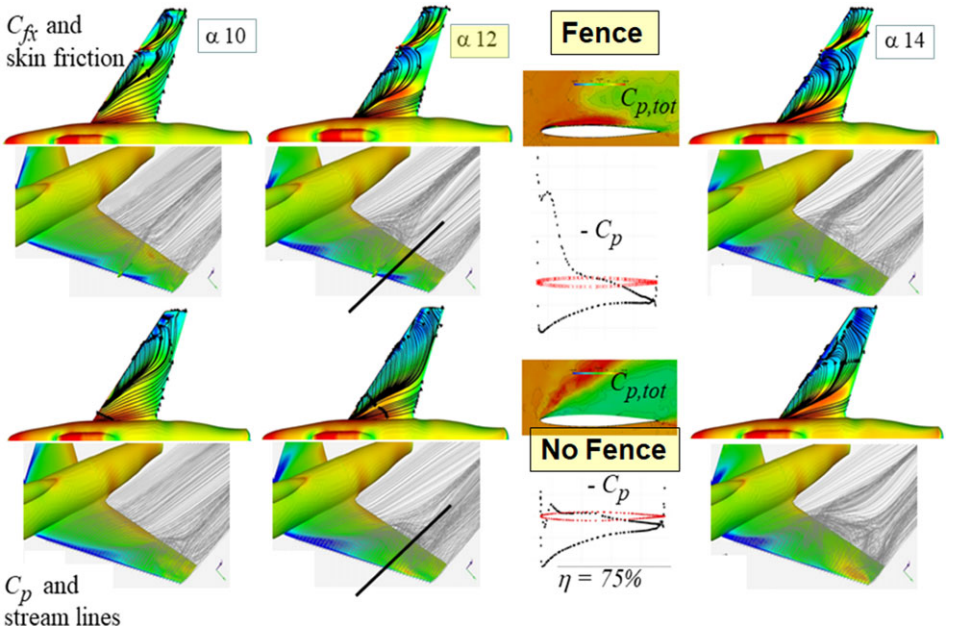

Figure 26. *Flow visualisation with streamlines and pressure coefficient over lower (port) wings, skin friction lines and x-component of skin friction coefficient over upper (starboard) wings. Inset with chordwise pressure distribution at 75% semi-span.*

6.2.2 Compare vortex effects: fence – no fence

To illustrate how the fence beneficially controls the vortex patterns, a series of RANS computations are made with the M-Edge code [73, 74]. The wing is computed with and without fence for different flow speeds and angles of attack. Figure 26 shows results at $M_\infty = 0.4$. The inset surface chordwise pressure profile at 75% semi-span shows the strongly increased lift created by the stall-fence stabilisation of the outboard flow. At $\alpha = 14°$ the fenceless wing has reverse, separated flow over the whole outer wing with low authority for the ailerons.

This exercise shows the cause and effect benefits of the wing fence as a device to mitigate the undesired consequences of wing sweep. The fence is just one of a number of such devices. For the J32 the Saab engineers also looked closely at leading-edge slats, whose benefits closely rivaled the wing fence. In order to decide which device should go into production, Saab built two prototypes: one with the wing fence, and the other with leading-edge slats. After careful evaluation of extensive flight testing of these two prototypes, the Saab engineers decided on the wing fence. This decision involved many trade-offs, not only aerodynamic ones, and shows how slim the margins are between the choices that aircraft designers must make.

7.0 Concluding remarks

The paper has been written with a view to describe by examples our current understanding of separated and vortical flow in aircraft wing aerodynamics, to show the simulation capabilities of computation methods of different modeling level, and to demonstrate and to explain the relevant flow phenomena. The cases discussed involve the aerodynamics of slender wing aircraft having flow patterns with coherent vortices over hybrid wings and wings of moderate sweep. Both cruise performance and stalling characteristics are influenced by strong vortex interactions. Two important elements of wing-flow physics have

https://doi.org/10.1017/aer.2023.39 Published online by Cambridge University Press

been discussed: separation from a smooth surface that creates a vortex, and vortex bursting, the abrupt breakdown of a vortex with a subsequent loss of lift.

Vortex aerodynamics of not-so-slender wings encounter particularly challenging problems, and it was shown how the design of early-generation aircraft surmounted these difficulties. Through use of forensic CFD, the article concludes with two case studies of aerodynamic design: how the Saab J29A wing maintains control authority near stall, and how the Saab J32 mitigates pitch-up instability at high incidence.

Modern RANS technology provides many useful predictions for attached flows as well as for flows with concentrated shed vortices. But vortex interaction with other vortices and breakdown lead to unsteady, largely separated turbulent flow which has been found out-of-scope for RANS. Direct simulation of the Navier-Stokes equations is out of computational reach in the foreseeable future, and the need for better physical modeling is evident.

The starting point would be hybrid RANS/LES simulation. Further understanding is needed on how to adequately resolve the relevant fluctuating turbulent phenomena in time and space. The separated flow region is extensive so appropriate gridding for the LES methodology becomes a critical issue. Such understanding can only come from systematic studies of all the factors involved for the accurate simulation of extensive separated turbulent flow, the real proof of the pudding.

More collaborative campaigns and concerted efforts will be needed, broken down into reduced complexity and even unit problems, to study the broader operating regimes of incoherent and extensive separation.

Acknowledgements. This author wishes to acknowledge the many fruitful discussions with two colleagues, Jesper Oppelstrup and Jim Luckring, that helped formulate the ideas and material presented on separation-induced leading-edge vortices and their effects on vortex-flow aerodynamics. The work on the two Saab planes, the J29 and the J32, would not have been possible without the support of Kenneth Nilsson, Tord Jonsson and Yngve Sedin at Veteranklubben Saab, and it is greatly appreciated. Lastly, the author wishes to thank Peter Eliasson and Mengmeng Zhang for carrying out the computations in the forensic CFD studies with the M-Edge code.

References

[1] Elsenaar A. Vortex formation and flow separation: The beauty and the beast in aerodynamics. *Aeronaut. J.*, 2000, **104**, (1042), pp 615–633.
[2] Luckring J. The discovery and prediction of vortex flow aerodynamics. *Aeronaut. J.*, 2019, **123**, (1264), pp 729–804.
[3] Lanchester F.W. *Aerodynamics, Constituting the First Volume of a Complete Work on Aerial Flight*. London: Archibald Constable & Co., 1907.
[4] Anderson J.D. *The Grand Designers: The Evolution of the Airplane in the 20th Century*. Cambridge, MA: Cambridge University Press, 2018.
[5] Jones M.B. The streamline aeroplane. *Aeronaut. J.*, 1929, **33**, (221), pp 357–385.
[6] Busemann A. Aerodynamischer Auftrieb bei Überschallgeschwindigkeit. *Proc. Volta Congress*, Rome 1935, pp 328–360, also Luftfahrtforschung, 1935, 12, pp 210–220.
[7] Meier H.U. (ed.) *German Development of the Swept Wing–1935–1945*. Reston, VA: Library of Flight, AIAA, 2010.
[8] Hirschel E.H., Rizzi A., Breitsamter C. and Staudacher W. *Separated and Vortical Flow in Aircraft Wing Aerodynamics*, Berlin: Springer-Verlag, 2021.
[9] Rizzi A. and Oppelstrup J. *Aircraft Aerodynamic Design with Computational Software*. Cambridge, MA: Cambridge University Press, 2021.
[10] Lippisch A. *The Delta Wing: History and Development*, Ames: Iowa State University Press, 1981.
[11] Küchemann D. Types of flow on swept wings. *J. Royal Aero Soc.*, 1953, **57**, (515), pp 683–699.
[12] https://su2code.github.io/
[13] Peake D.J. and Tobak M. Three-dimensional interaction and vortical flows with emphasis on high speeds. NASA TM 81169, 1980 and *AGARDograph 252,* 1980
[14] Küchemann D. Report on the lUTAM symposium on concentrated vortex motion in fluids. *J. Fluid Mech.*, 1965, **21**, pp 1–20.
[15] Gibbs-Smith C.H., *The Invention of the Aeroplane 1799–1909*. London: Taplinger Publishing, 1966.
[16] Munk M.M. Isoperimetrische Probleme aus der Theorie des Fluges. Göttingen dissertation, 1918. Also *NACA Report 121*, 1923.
[17] Anderson J.D. *A History of Aerodynamics and Its Impact on Flying Machines*. Cambridge, MA: Cambridge University Press, 1999, Chapter 6, pp 246–247.
[18] Kutta M.W. Auftriebskräfte in strömenden Flüssigkeiten. *Illustrierte Aeronautische Mitteilungen*, 1902, **6**, pp 133–135.

https://doi.org/10.1017/aer.2023.39 Published online by Cambridge University Press

[19] Prandtl L., Uber Flüssigkeitsbewegung bei sehr kleiner Reibung, Verhandlungen des dritten Internationalen Mathematiker, Kongresses in Heidelberg, 1904. Also *NACA Technical Memorandum* No. 452, 1928.
[20] Joukowski N.E. On annexed vortices. *Proc. Phys. Sect. Nat. Sci. Soc.*, 1906, **13**, p 12.
[21] Joukowski N.E. *Geometrische Untersuchungen über die Kutta'sche Strömung, (Trans) Physical Section of the Imperial Society of the Friends of Natural Science*, Moscow, 1910/1912.
[22] Prandtl L. Tragflügeltheorie I. *Mitteilungen von der Gesellschaft der Wissenschaften zu Göttingen*, 1911.
[23] Prandtl L. Tragflügeltheorie II. *Mitteilungen von der Gesellschaft der Wissenschaften zu Göttingen*, 1918.
[24] Von Karman T. *Aerodynamics, Selected Topics in the Light of Their Historical Development*. Ithaca, NY: Cornell University Press, 1957.
[25] Prandtl L. The generation of vortices in fluids of small viscosity. *J. Royal Aeronaut. Soc.*, 1927, **31**, pp 718–741.
[26] Lewin K. *Field Theory in Social Science: Selected Theoretical Papers by Kurt Lewin*, London: Tavistock, 1952.
[27] Jarrett P. F.W. Lanchester and the great divide. *J. Aeronaut. Hist.*, Paper No. 2014/02, 2014, https://www.aerosociety.com/media/4846/fw-lanchester-and-the-great-divide.pdf
[28] Lanchester, F.W. The Wright and Voisin types of flying machine. A comparison. *Aeronaut. J.*, 1909, **XIII**, (49), pp 4–12.
[29] Bloor D. *The Enigma of the Aerofoil: Rival Theories in Aerodynamics, 1909–1930*, Chicago: University of Chicago Press, 2011.
[30] https://www.maths.cam.ac.uk/about/history
[31] Fage A. and Simmons L.F.G., An investigation of the air-flow pattern in the wake of an aerofoil of finite Span. *Philos. Trans. Royal Soc. London, Series A*, 1926, **225**, pp 303–330.
[32] Goldstein S. Hydrodynamics: Book review, *The Mathematical Gazette*, 1933, **17**, (224), pp 215–217.
[33] Hansen J.R. *Engineer in Charge: A History of the Langley Aeronautical Laboratory, 1917–1958, NASA SP-4305*. Washington, DC: NASA, 1987.
[34] Rolls L.S. and Matteson F.H. Wing load distribution on a Swept-wing airplane in flight at Mach Numbers Up to 1.11, and comparison with theory. NACA RM A52A31, 1952.
[35] Rizzi A. and Luckring J. Historical development and use of CFD for separated flow simulations relevant to military aircraft. *Aerosp. Sci. Technol.*, 2021, **117**, pp 1–42.
[36] Rubbert P.E. *Theoretical Characteristics of Arbitrary Wings by a Nonplanar Vortex Lattice Method, Boeing Report D6-9244*: The Boeing Company, 1964.
[37] Hedman S.G. *Vortex Lattice Method for Calculation of Quasi Steady State Loadings on Thin Elastic Wings in Subsonic Flow*. Stockholm: FFA the Aeronautical Research Institute of Sweden Report 105, 1966.
[38] Rizzi A. and Engquist B. Selected topics in the theory and practice of computational fluid dynamics. *J. Comp. Phys.*, 1987, **72**, pp 1–69.
[39] Vos J.B., Rizzi A., Darracq D. and Hirschel E.H. Navier-Stokes solvers in European aircraft design. *Progr. Aerosp. Sci.*, 2002, **38**, (8), pp 601–697.
[40] Spalart P.R., Jou W-H., Strelets M. and Allmaras S.R. Comments on the feasibility of LES for Wings, and on a Hybrid RANS/LES approach. In *Advances in DNS/LES, 1st AFOSR Int. Conf. on DNS/LES*, Columbus, OH: Greyden Press, 1997.
[41] Rizzi A. and Henningson D. Aeronautical CFD and turbulence – Progress and challenges. *ICAS Paper 2022-0104*, 2022, pp 1–23.
[42] https://www.ercoftac.org/publications/ercoftac_best_practice_guidelines
[43] Örnberg K.T. Way of dividing the vortex system on a wing and devices to do this, (in Swedish), Sweden Patent Klass 62 b:4/04, No 160134, 1953.
[44] Örnberg K.T. Stabilizing the vortices over a thin delta wing. *U.S. Patent*, 1969, **3**,(471), p 107.
[45] Palme H.O. Summary of Stalling characteristics and maximum lift of Wings at low speeds. Saab Technical Notes TN-15, Linköping, 1953.
[46] Shortal J. and Maggin B. Effects of Sweepback and aspect ratio on longitudinal stability characteristics of Wings at low speeds. *NACA TN* 1093, 1946.
[47] Furlong C. and McHugh J.G. Analysis of the low-speed longitudinal characteristics of Swept Wings at high Reynolds number. *NACA Report* 1339, 1952.
[48] Polhamus E.C. A survey of Reynolds number and Wing geometry effects on lift characteristics in the low speed stall region. *NASA CR* 4745, 1996.
[49] Visbal M.R. and Garmann D.J. Dynamic stall of a finite-aspect-ratio wing. *AIAA J.*, 2019, **57**, (3), pp 962–977.
[50] Visbal M.R. and Garmann D.J. Effect of Sweep on dynamic stall of a pitching finite-aspect-ratio Wing. *AIAA J.*, 2019, **57**, (8), pp 3274–3289.
[51] Spalart P.R. and Venkatakrishnan V. On the role and challenges of CFD in the aerospace industry. *Aeronaut. J.*, 2016, **120**, (1223), pp 209–232.
[52] Levy D.W. and DPW Organizing Committee. The CFD Drag prediction workshop series: Summary and retrospective, https://cfd.ku.edu/JRV/Levy.pdf
[53] Elmiligui A., Abdol-Hamid K., Cavallo P.A. and Parlette E.B. USM3D simulations for the F-16XL aircraft configuration. *J. Aircraft*, 2017, **54**, (2), pp 417–427. Also *AIAA Paper* 2014-0756, 2014.
[54] Morton S.A. and McDaniel D.R. F-16XL simulations at flight conditions using hybrid near- body/offbody computational fluid dynamics. *J. Aircraft*, 2017, **54**, (6), pp 2050–2069. Also AIAA Paper 2015-2873, 2015.
[55] Lofthouse A.J. and Cummings R.M. Numerical simulations of the F-16XL at flight-test conditions using delayed detached-Eddy simulation. *AIAA J. Aircraft*, 2017, **54**, (6), pp 2077–2099. Also AIAA Paper 2015-2875, 2015.

https://doi.org/10.1017/aer.2023.39 Published online by Cambridge University Press

[56] Luckring J.M. Introduction to the special section on F-16XL flight aerodynamics predictions at a high angle of attack. *J. Aircraft*, 2017, **54**, (6), p 2013.
[57] Lambourne N.C. and Bryer D.W. The bursting of leading edge vortices – some observations and discussion of the phenomenon. *ARC R&M 3282*, 1962.
[58] Görtz S. Realistic simulations of delta wing aerodynamics using novel CFD methods, KTH PhD dissertation. Rep Trita-AVE 2005:01, Stockholm, 2005.
[59] RTO. Vortex Breakdown over Slender Delta Wings, *RTO-TR-AVT-080*, 2009.
[60] Gordnier R.E. Numerical simulation of a 65-degree delta Wing Flowfield. *J. Aircraft*, 1997, **34**, (4), pp 492–499.
[61] Poll D.I.A. Spiral Vortex flow over a Swept-Back Wing. *Aeronaut. J.*, 1986, **90**, pp 185–199.
[62] STO. Reliable prediction of separated flow onset and progression for air and sea vehicles. STO-TR-AVT-183, 2017.
[63] RTO. Assessment of stability and control prediction methods for NATO air and sea vehicles. RTO-TR-AVT-161, 2012.
[64] Frink N.T., Tomac M. and Rizzi A. Collaborative study of incipient separation on 53°-swept diamond wing. *Aerosp. Sci. Technol.*, 2016, **57**. Also AIAA paper 2015-0288, 2015.
[65] Black J. Flow studies of the leading edge stall on a swept-back wing at high incidence. *J. Royal Aeronaut. Soc.*, 1956, **60**, pp 51–60.
[66] Cummings R. and Schütte A. Integrated computational/experimental approach to unmanned combat air vehicle stability and ontrol estimation. *J. Aircraft*, 2012, **49**, (6), pp 1542–1557.
[67] Eliasson P., Rizzi A., Oppelstrup J. and Zhang M., Improving Stall characteristics of UCAV Wing with Vortex generators. *ICAS Paper 2022-0238*, 2022, pp 1–9.
[68] Coppin J., Birch T, Kennet D., Hoholis G. and Badcock K. Prediction of control effectiveness for a highly Swept unmanned air vehicle configuration. *J. Aircraft*, **55**, (2), 2018, pp 534–548.
[69] Schütte A., Hummel D. and Hitzel S.M. Flow physics analyses of a generic unmanned combat aerial vehicle configuration. *J. Aircraft*, 2012, **49**, (6), pp 1638–1651.
[70] Hövelmann A.N. Analysis and control of partly-developed leading-edge vortices, PhD Thesis, Technical University of München, 2016.
[71] Furlong C. and McHugh J.G. Analysis of the low-speed longitudinal characteristics of Swept Wings at high Reynolds number. NACA Report 1339, NACA, 1952.
[72] Petersohn E. *Vindtunnelundersökning av Fpl typ R1001. Undersökning vid låga hastigheter, FFA Rapport Nr AU-93:1 (in Swedish)*. Sweden: Bromma, 1946.
[73] Eliasson P. and Weinerfelt P. Recent applications of the flow Solver edge. *Proceedings of 7:th Asian CFD Conference*, Bangalore, India, 2007.
[74] Eliasson P., Weinerfelt P. and Bramkamp F. Enhancing CFD predictions for the Gripen Aircraft, *ICAS Paper 2022-0242*, 2022, pp 1–16.

Cite this article: Rizzi A. (2023). Separated and vortical flow in aircraft aerodynamics: a CFD perspective. *The Aeronautical Journal*, **127**, 1065–1103. https://doi.org/10.1017/aer.2023.39